Development 134, 611-623 (2007) doi:10.1242/dev.02749

Specification of epibranchial placodes in zebrafish

Alexei Nechiporuk[1], Tor Linbo[1], Kenneth D. Poss[2] and David W. Raible[1,*]

In all vertebrates, the neurogenic placodes are transient ectodermal thickenings that give rise to sensory neurons of the cranial ganglia. Epibranchial (EB) placodes generate neurons of the distal facial, glossopharyngeal and vagal ganglia, which convey sensation from the viscera, including pharyngeal endoderm structures, to the CNS. Recent studies have implicated signals from pharyngeal endoderm in the initiation of neurogenesis from EB placodes; however, the signals underlying the formation of placodes are unknown. Here, we show that zebrafish embryos mutant for *fgf3* and *fgf8* do not express early EB placode markers, including *foxi1* and *pax2a*. Mosaic analysis demonstrates that placodal cells must directly receive Fgf signals during a specific crucial period of development. Transplantation experiments and mutant analysis reveal that cephalic mesoderm is the source of Fgf signals. Finally, both Fgf3 and Fgf8 are sufficient to induce *foxi1*-positive placodal precursors in wild-type as well as Fgf3- plus Fgf8-depleted embryos. We propose a model in which mesoderm-derived Fgf3 and Fgf8 signals establish both the EB placodes and the development of the pharyngeal endoderm, the subsequent interaction of which promotes neurogenesis. The coordinated interplay between craniofacial tissues would thus assure proper spatial and temporal interactions in the shaping of the vertebrate head.

KEY WORDS: Fgf3, Fgf8, Foxi1, Pax2a, Epibranchial placodes, Cranial ganglia, Cephalic mesoderm, Zebrafish

INTRODUCTION

In vertebrates, placodes are transient epithelial thickenings within non-neural ectoderm that give rise to sensory neurons of the cranial ganglia as well as the lens and sensory structures of the nose and ear. The neurogenic placodes include trigeminal placodes that form neurons of the trigeminal ganglia, and epibranchial (EB) placodes that generate sensory neurons of the distal facial, glossopharyngeal, and vagal ganglia. EB neurons innervate internal organs to transmit information such as heart rate, blood pressure, and visceral distension from the periphery to the CNS. In zebrafish, the EB placodes are positioned ventrally to the ear at the dorsal aspect of the pharyngeal arches: the facial placode is associated with the second arch, the glossopharyngeal with the third, and four vagal placodes with the four posterior-most arches. Despite their functional importance and evolutionary conservation, the signals underlying neurogenic placode induction are not known.

EB placode induction is likely to be a multi-step process (Streit, 2004). A growing body of evidence suggests that along with the various other placodes, EB placodes are derived from a common territory, named pre-placodal or panplacodal ectoderm (PPE), positioned around the border of the anterior neural plate. PPE is defined by expression of specific transcription factors, including the homeobox factor Six1 and its binding partner Eya1 (Bessarab et al., 2004; Pandur and Moody, 2000; Sahly et al., 1999; Schlosser and Ahrens, 2004; Zou et al., 2004). Initial formation of the PPE is regulated by Bmp, Wnt and Fgf signals (Ahrens and Schlosser, 2005; Brugmann et al., 2004; Litsiou et al., 2005). Transplantation and fate-mapping studies support the idea that the PPE represents the earliest stage in placode induction (Jacobson, 1963; Kozlowski et al., 1997; Martin and Groves, 2006; Streit, 2002). Initially, cells destined to form EB placode are intermingled within the PPE with precursors of the otic placode (Streit, 2002) in what may be a PPE subdomain (Schlosser and Ahrens, 2004). Cells then segregate via an unknown mechanism to form EB placodes. Once placodes are formed, Fgf3 and Bmp signal from the endodermal pouches to induce neurogenesis (Begbie et al., 1999; Holzschuh et al., 2005; Nechiporuk et al., 2005; Trokovic et al., 2005).

Different stages of EB placode development are revealed by transcription factor expression. Foxi1 is a forkhead-related winged helix transcription factor expressed in EB placode precursors, and in *foxi1* mutants, placodal progenitors fail to undergo neurogenesis and subsequently die (Lee et al., 2003). Pax2 is a paired domain transcription factor that is upregulated in the EB placodes in chick and *Xenopus* prior to neurogenesis (Baker and Bronner-Fraser, 2000; Schlosser and Ahrens, 2004). *ngn1* (also known as *neurog1* – Zebrafish Information Network) is the earliest proneural gene expressed in zebrafish EB placodes (Andermann et al., 2002). Similarly, *neurogenin* genes are expressed in EB placodes in other species (Fode et al., 1998; Schlosser and Ahrens, 2004). In zebrafish, Ngn1 activity is required for expression of *phox2a* and *phox2b* (Nechiporuk et al., 2005), homeobox transcription factors that are in turn necessary for subsequent differentiation of EB neurons (Dauger et al., 2003).

Although signals that regulate EB placode formation are unknown, Fgf signals are required for otic placode development in zebrafish, chick and mouse (Ladher et al., 2005; Leger and Brand, 2002; Liu et al., 2003; Maroon et al., 2002; Wright and Mansour, 2003). Loss-of-function experiments in zebrafish demonstrated that Fgf3 and Fgf8 are redundantly required at multiple stages of otic placode induction (Leger and Brand, 2002; Solomon et al., 2004). Foxi1 is necessary during otic placode induction and at that point *foxi1* expression is independent of Fgf signals (Nissen et al., 2003; Solomon et al., 2003; Solomon et al., 2004). In contrast, we have previously shown that Fgf signaling is necessary to maintain expression of *foxi1* in EB placodal precursors, suggesting that Fgf signals might also be important for early specification of EB placodes (Nechiporuk et al., 2005).

In this study, we show that global disruption of Fgf signaling blocks EB placode induction and subsequent neurogenesis. Using transplantation techniques, we demonstrate that Fgf signaling is required cell autonomously in EB placodes. Analyses of zebrafish

[1]Department of Biological Structure, University of Washington, Seattle, WA 98195-7420, USA. [2]Department of Cell Biology, Duke University Medical Center, Durham, NC 27710, USA.

*Author for correspondence (e-mail: draible@u.washington.edu)

Accepted 20 November 2006

mutants strongly suggest that inducing signals are mesoderm-derived, and that two mesodermally expressed *fgf* genes, *fgf3* and *fgf8*, are required for EB placode formation. Transplantation of wild-type mesoderm into *fgf3+8* morphants rescues EB ganglia, and ectopic Fgf3 or Fgf8 are sufficient to induce *foxi1*-positive EB precursors and *phox2b*-positive EB neurons. Overall, our results revealed a combined role for Fgf3 and Fgf8 during EB placode induction, and suggest a model where interactions between cranial mesoderm, ectoderm and endoderm are coordinated to assure proper development of the vertebrate head.

MATERIALS AND METHODS

Fish care, fish strains, SU5402 and heat-shock treatments

Wild-type embryos were obtained from natural spawning of *AB adults and staged by age (hours post-fertilization (hpf) at 28.5°C) and morphological criteria (Kimmel et al., 1995). The following alleles were used to produce mutant embryos: *fgf8, ace*^{ti282a} (Reifers et al., 1998); *foxi1*, *hsy*^{em1} (Solomon et al., 2003); *fgf3, lia*^{t24149} (Herzog et al., 2004); and *pax2a, noi*^{tu29a} (Lun and Brand, 1998). Maternal-zygotic *one-eyed pinhead* (*MZoep*) embryos were generated by crossing adult *oep*^{tz57} mutant fish, which had been rescued by injecting 20 pg of *oep* mRNA at the one-cell stage (Gritsman et al., 1999). The Fgfr inhibitor, SU5402 (Calbiochem), was dissolved in dimethyl sulfoxide (DMSO) at 50-100 mM and then further diluted to a working concentration in embryo medium (EM) (Westerfield, 2000). Control embryos were treated with the same amount of DMSO in EM. Embryos treated with a 60 μmol/L solution lacked trunk mesoderm, otic vesicle, and *erm* and *pea3* expression, without exhibiting significant cell death. Thus, we used 60 μmol/L concentration in all our subsequent treatments. To obtain *hsp70::dn-fgfr1*-positive embryos we crossed [*Tg(hsp70::dn-fgfr1)*]^{pd1} heterozygotes (Lee et al., 2005) to wild-type fish, heat shocked embryos at 38.5°C for 30 minutes and sorted embryos 2-12 hours later using epifluorescence. GFP-negative embryos were used as controls.

Generation of *phox2b::egfp* transgenic line

We modified a *phox2b*-containing bacterial artificial chromosome (BAC) clone by *Escherichia coli*-based homologous ET-recombination (Zhang et al., 1998). BAC clone C192B19 contains approximately 92 kb of sequence upstream and 32 kb downstream of *phox2b* (http://www.sanger.ac.uk/Projects/D_rerio/mapping.shtml). Following recombination, the modified BAC clone contained an *egfp* gene positioned at an endogenous start site. The accuracy of recombination was evaluated by PCR, sequencing, and by transient expression assays. *phox2b::egfp* BAC faithfully recapitulated endogenous *phox2b* expression in cranial ganglia and other organs. To obtain a germline, we injected linearized BAC DNA into zebrafish embryos, raised injected fish to adulthood, and screened their progeny for reporter gene expression. The germline transmission rate was 3%. The [*Tg(phox2b::egfp)*]^{w37} strain has been outcrossed for two generations and transmitted the transgene in a Mendelian fashion.

Morpholino injections

Antisense morpholino oligonucleotides (MO) were obtained from GeneTools (Corvalis, OR), diluted to a working concentration in Danieau buffer (58 mmol/L NaCl, 0.7 mmol/L KCl, 0.4 mmol/L $MgSO_4$, 0.6 mmol/L $Ca(NO_3)_2$, and 5 mmol/L HEPES, pH 7.6), and 2-3 nL were pressure-injected into one- or two-cell stage embryos. *cas*-MO, 5′-GCAT-CCGGTCGAGATACATGCTGTT, was injected at 2 ng/nL (Sakaguchi et al., 2001); *fgf3*-MO, 5′-CATTGTGGCATGGAGGGATGTCGGC, was injected at 0.75 ng/nL (Maroon et al., 2002); *fgf8*-MOE2I2+*fgf8*-MOE3I3, 5′-TAGGATGCTCTTACCATGAACGTCG+5′-CACATACCTTGCCAA-TCAGTTTCCC, were injected at 2+2 ng/nL each (Draper et al., 2001).

In-situ hybridization and immunolabeling

In-situ hybridization and immunolabeling experiments were performed according to the published protocols (Andermann et al., 2002). We used the following riboprobes and antibodies: *erm* (Raible and Brand, 2001; Roehl and Nusslein-Volhard, 2001), *eya1* (Sahly et al., 1999), *fgf3* (Kiefer et al., 1996), *fgf8* (Reifers et al., 1998), *fgfr1* (Scholpp et al., 2004), *fgfr2* (Tonou-Fujimori et al., 2002), *foxi1* (Lee et al., 2003; Nissen et al., 2003; Solomon et al., 2003), *ngn1* (Korzh et al., 1998), *nkx2.3* (Lee et al., 1996), *pax2a* (Krauss et al., 1991), *pea3* (Raible and Brand, 2001; Roehl and Nusslein-Volhard, 2001), *phox2a* (Guo et al., 1999), *phox2b* (Shepherd et al., 2004), anti-Hu (1:750, Sigma), anti-Pax2 (1:100, COVANCE), anti-Prox1 (1:1000, Chemicon). For brightfield photography, embryos were deyolked when appropriate, flat mounted in 50% glycerol plus 50% PBS and photographed on a Nikon SMZ 1500 stereoscope or Zeiss Axioplan microscope using Spot CCD camera (Diagnostic Instruments). Fluorescent images were obtained using an LSM-5 Pascal confocal microscope (Zeiss). Brightness and contrast were adjusted using Adobe Photoshop. Plastic sections of 5-6 μm were obtained from in situ-stained embryos. For red Linbo's counterstain, dry slides were treated with 0.5 mol/L NaOH for 5 minutes at room temperature, then washed four times in water and dried at 73°C. Heated slides were immersed into 2% solution of Basic Fuchsin (Allied Chemical Corporation) for 2 minutes, washed four times in water, dried and coverslipped.

Transplantation experiments

For transplants, embryos were raised in filtered EM supplemented with penicillin (5000 U/L)/streptomycin (100 mg/L; Sigma). Donor embryos were injected at the one-cell stage with 2% lysine-fixable fluorescein or tetramethylrhodamine dextran (10,000 M_r; Molecular Probes) in 0.2 mol/L KCl. Dechorionated donor and host embryos were mounted in 3.2% methylcellulose in EM on a glass depression slide. For targeted transplants, 25-30 donor cells were inserted into the presumptive placodal domain of a shield-staged host embryo, about 40° from the margin and 110° from the shield. For mesodermal transplants, 25-30 cells were laid around the margin of a 30-40% epiboly-staged embryo. Donor-derived fluorescein-labeled cells were detected essentially as described (Nechiporuk et al., 2005).

Fgf3 and Fgf8 misexpression

hs-fgf3myc (Maves et al., 2002), *hs-fgf8* (Roehl and Nusslein-Volhard, 2001) and *hs-gfp* plasmids were injected into one-cell- or two-cell-staged embryos at 2.5 ng/μL. Embryos were heat-shocked at 38.5°C for 30 minutes between 10 and 16 hpf, fixed at various time points and processed to detect *foxi1* or *pax2a* mRNA. To detect Fgf-myc or GFP expression following RNA in-situ hybridization, embryos were processed with mouse monoclonal anti-Myc (1:1000; Cell Signaling) or rabbit polyclonal anti-GFP antibody (1:1000, Molecular Probes), and Alexa 568 or Alexa-488 secondary antibody (1:1000, Molecular Probes) as described (Andermann et al., 2002).

Bead-implantation experiments were performed essentially as described (Maves et al., 2002). Briefly, 20 μm polystyrene beads (Polysciences) were rinsed in PBS, treated with 0.5 mg/mL heparin for 20 minutes at room temperature, then incubated in 250 μg/mL mouse FGF8b (R&D Systems) with 0.5% bovine serum albumin (BSA) in PBS for 2 hours at room temperature. Control beads were incubated in 0.5% BSA in PBS. Embryos were mounted similar to transplantation experiments. A small incision was made with a glass needle approximately half way between the first somite and the anterior limit of the neural plate. One to three beads were placed under the ectoderm either lateral to or into the neural plate tissue. To test the efficacy of FGF8b beads, embryos with implanted beads were stained for *pea3* (Raible and Brand, 2001; Roehl and Nusslein-Volhard, 2001). In total, 15 out of 17 embryos showed a ring of *pea3* expression around the FGF8b bead.

RESULTS

pax2a is expressed in zebrafish EB placodes prior to neurogenesis

To assess initial EB placode formation, we searched for markers that are upregulated in placodes before the onset of neurogenesis at 24 hpf. As Pax2 is expressed in the EB placodes in chick and *Xenopus* (Baker and Bronner-Fraser, 2000; Schlosser and Ahrens, 2004), we analyzed its expression in zebrafish (see Fig. S1A in the supplementary material). Expression of *pax2a* is found in presumptive facial placodes beginning at 16-18 hpf (see Fig. S1A in the supplementary material; data not shown) and extends caudally to include presumptive glossopharyngeal and vagal placodes between 20-24 hpf. Transverse sections of 24-hour-old embryos

revealed *pax2a* mRNA in thickened columnar placodal epithelium (see Fig. S1A in the supplementary material, arrows) but only in its ventral part (see Fig. S1A in the supplementary material, arrowheads). Between 28 and 36 hpf, *pax2a* expression is maintained in individual placodes and in internalized neuroblasts, but downregulated in differentiated Hu-positive EB neurons (see Fig. S1B in the supplementary material; data not shown). The zebrafish *pax2a* null mutant *no isthmus* (*noi*^{tu29a}) (Lun and Brand, 1998) displayed about 50% reduction in EB neurons (see Fig. S1C in the supplementary material). Foxi1 activity is required for *pax2a* expression; *pax2a* message was absent or strongly reduced in *foxi1* mutant embryos (see Fig. S1D in the supplementary material). Altogether these data indicate that *pax2a* is expressed in the EB placodes prior to and during neurogenesis and is necessary for their development.

Fgf signaling is required for EB placode induction

To analyze the role of Fgf signaling in EB placode induction, we examined *foxi1*, *pax2a*, and *phox2b* expression in zebrafish embryos treated with a Fgf receptor (Fgfr) inhibitor, SU5402 (Fig. 1) (Mohammadi et al., 1997). Zebrafish embryos were incubated with SU5402 or DMSO (control) beginning at 10 hpf. Alternatively, we used a zebrafish transgenic line that carries a heat-shock-inducible form of dominant-negative Fgfr1 fused to GFP (*hsp70::dn-fgfr1*) (Lee et al., 2005). *foxi1* expression was strongly reduced at 19 hpf in both SU5402 and *hsp70::dn-fgfr1* embryos (Fig. 1). *pax2a* expression in the EB placodes was completely absent at 24 hpf, and *phox2b* expression was either absent or strongly reduced at 36 hpf (Fig. 1). Thus, Fgf signaling is required for expression of early placodal markers and subsequent neurogenesis.

We used the SU5402 inhibitor and the *hsp70::dn-fgfr1* transgenic line to determine the temporal requirement for Fgf signaling. In zebrafish the SU5402 block is reversible, with Fgf-mediated signaling restored within 1-2 hours after the inhibitor removal (Crump et al., 2004; Maroon et al., 2002; Phillips et al., 2001). We incubated embryos in SU5402 for periods of 1.5-4.5 hours, and analyzed them at 24 hpf using Pax2 antibody (Fig. 2A). In parallel, *hsp70::dn-fgfr1* embryos were heat shocked at the same time points as for inhibitor application (Fig. 2B,C). In both sets of experiments, Pax2 expression in the facial placode was either absent or strongly reduced when Fgf signaling was inhibited between the 10- and 16.5-hour stages, with the strongest requirement found between 10 and 11.5 hpf. Pax2 expression in the glossopharyngeal and vagal placodes was most strongly affected later, after 11.5 hpf, suggesting that the EB placodes are induced in an anterior to posterior fashion. Together, these experiments demonstrate a strong Fgf requirement between 10 and 16.5 hpf for all EB placodes (Fig. 2C), well before the onset of neurogenesis at 24 hpf.

To determine whether Fgf signaling is active in EB placode precursors, we analyzed expression of *fgf* receptors, and the Fgf transcriptional targets *erm* and *pea3* (see Fig. S2 in the supplementary material). Fgfr1 has been suggested to mediate Fgf8 signals (Scholpp et al., 2004), whereas *erm* and *pea3* are activated in response to both Fgf8 and Fgf3 (Raible and Brand, 2001; Roehl and Nusslein-Volhard, 2001). Transverse sections through 13-14-hour-old embryos revealed that *fgfr1*, *erm* and *pea3* are expressed in the ectoderm in presumptive EB placode precursors (see Fig. S2 in the supplementary material). In contrast, *fgfr2, fgfr3 and fgfr4* were not differentially expressed in the ectoderm at this stage (see Fig. S2 in the supplementary material; data not shown). Overall, these data demonstrate that Fgf signaling is active in EB placode precursors and is required for placode formation.

Fgf signaling is required cell autonomously in EB placodes

Both drug treatment and the *hsp70::dn-fgfr1* transgene expression globally block Fgf signaling throughout the embryo. We therefore generated mosaic embryos with cells from wild-type and *hsp70::dn-fgfr1* lines to determine which tissue(s) required receipt of the Fgf signal for proper EB placode formation. We labeled *hsp70::dn-fgfr1* donor embryos with fluorescein-dextran tracer and transplanted 25-30 cells to the prospective placodal domain of a wild-type host embryo at shield stage (Fig. 3A). Resulting embryos were heat shocked between 10 and 11 hpf and analyzed for Pax2 expression at 24 hpf. Whereas wild-type cells readily contributed to EB placodes in wild-type host embryos, *hsp70::dn-fgfr1* cells were largely

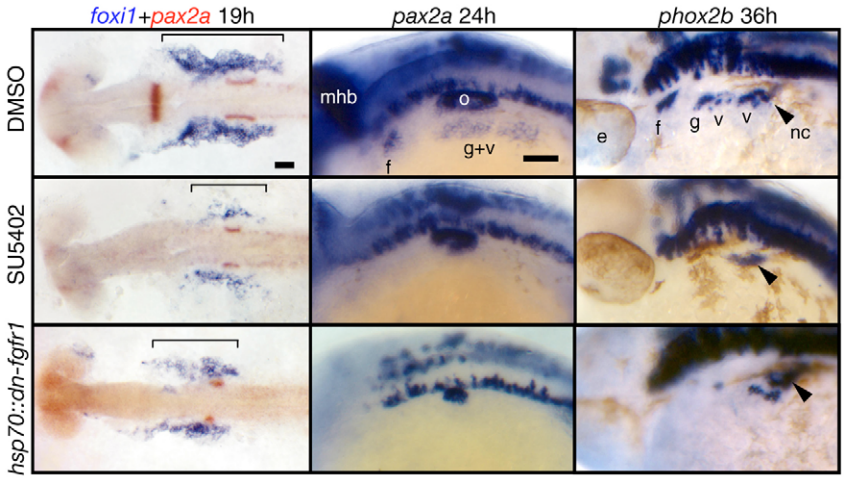

Fig. 1. Fgf signaling is required for EB placode development. *hsp70::dn-fgfr1* embryos (bottom panels) were heat shocked at 10 hpf (bud stage), collected at 19, 24 and 36 hpf and processed for in-situ hybridization with *foxi1*, *pax2a* and *phox2b*, respectively. Top and middle panels show embryos treated with the DMSO and the Fgfr inhibitor SU5402, respectively, beginning at 10 hpf and processed in the same way as the *hsp70::dn-fgfr1* embryos. All panels are lateral views, except *foxi1+pax2a* panels that show dorsal views. Anterior is at left. As expected, *pax2a* expression in the midhindbrain boundary and the otic vesicle was either absent or strongly reduced in the Fgf-depleted embryos. In the SU5402-treated and *hsp70::dn-fgfr1* embryos, *foxi1* expression is strongly reduced (bracket), and *pax2a* expression in the EB placodes is absent. *phox2b* was not expressed in EB placodes in SU5402-treated embryos; its expression was strongly reduced in *hsp70::dn-fgfr1* embryos, but a few *phox2b*-positive neurons remain in the large vagal ganglion. We presume that this milder phenotype resulted from the degradation of the transgenic protein. Black arrowheads mark the *phox2b*+ vagal neural crest cells (not affected in Fgf-depleted embryos) on their ventral migration route just posterior to the last branchial arch. These cells can be easily identified, because they make a characteristic turn toward the gut (Shepherd et al., 2004). Scale bars: 50 μm. e, eye; f, facial placode or ganglion; g, glossopharyngeal placode or ganglion; mhb, midhindbrain boundary; nc, vagal neural crest; o, otic vesicle; v, vagal placode or ganglion.

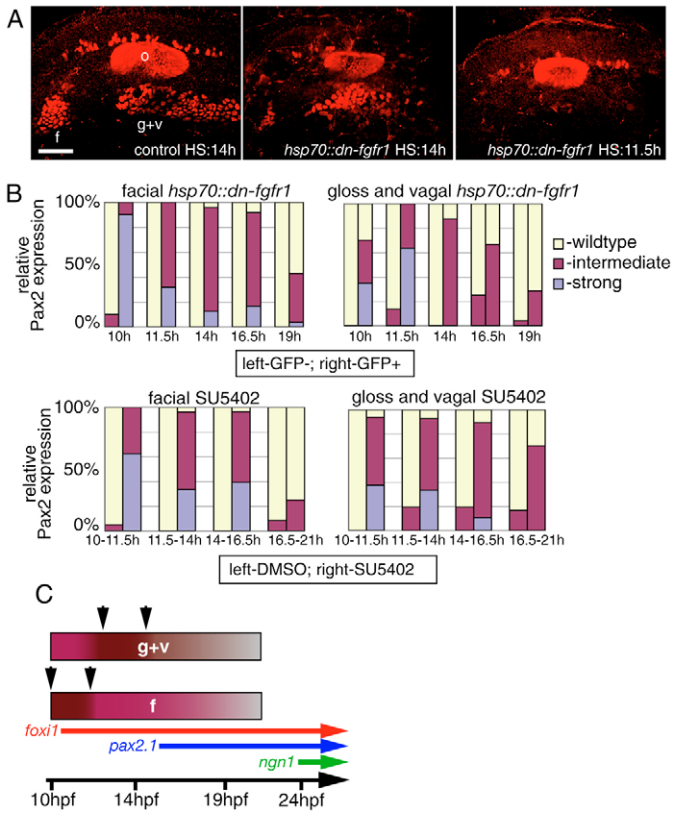

Fig. 2. Temporal requirement for FGF signaling. (**A**,**B**) Wild-type embryos were incubated for 1.5–4.5 hours in SU5402 starting at 10, 11.5, 14 and 16.5 hpf (DMSO-treated embryos were used as controls); heterozygous *hsp70::dn-fgfr1* fish were crossed to wild type and their progeny was heat shocked at the same time points (GFP-negative embryos were used as controls). In both cases, resulting embryos (6-14 per each time point) were analyzed using Pax2 antibody at 24 hpf and scored for either presence (A, left), reduction (A, middle), or absence (A, right) of the facial (B, left) and glossopharyngeal and vagal (B, right) placodes. (**C**) Summary of the data in (B). Note that Fgf signaling is strongly required between 10 and 11.5 hpf in the facial placode (f, arrows) and between 11.5 and 14 hpf in the glossopharyngeal and vagal placodes (g+v, arrows), implying that the EB placodes are formed in a rostral to caudal sequence. Scale bars: 50 μm. Abbreviations are as in Fig. 1.

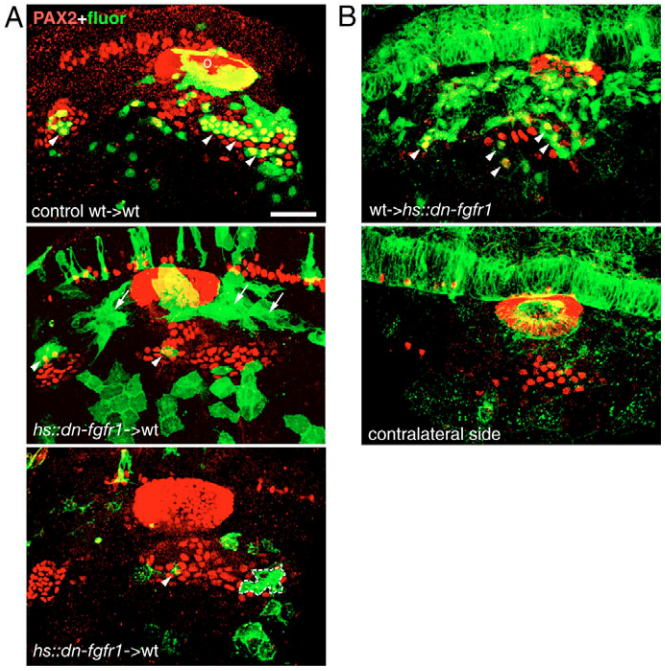

Fig. 3. Fgf signaling is required cell autonomously in EB placodes. (**A**) *hsp70::dn-fgfr1* donor embryos were injected with a lineage tracer (fluorescein-dextran, green). At shield stage, 25-30 donor cells were transplanted into the prospective placodal domain of wild-type hosts. Mosaic embryos were heat shocked at 10-11 hpf, collected at 24 hpf and analyzed for Pax2 protein expression (red). Panels show side view of the embryos that received either wild-type (A, top) or *hsp70::dn-fgfr1* cells (A, middle and bottom). Wild-type cells readily contributed to the EB placodes (arrowheads), whereas *hsp70::dn-fgfr1* cells either accumulated dorsally (arrows) or were excluded from EB placodes (A, bottom). Dotted line indicates a patch of *hsp70::dn-fgfr1* cells within the EB placode that did not express Pax2. (**B**) In reciprocal experiments, wild-type donor embryos were injected with a lineage tracer (fluorescein-dextran, green). At shield stage, 25-30 donor cells were transplanted into the prospective placodal domain of *hsp70::dn-fgfr1* hosts, mosaic embryos were heat shocked at 13.5-16 hpf, collected at 24 hpf and analyzed for Pax2 protein expression (red). Because dn-Fgfr1 protein is localized to the membrane, while fluorescein is evenly distributed throughout the cell, wild-type donor cells were easily distinguishable in the transgenic host embryos. Most of the GFP in the host is not visible (except hindbrain), because the image brightness and contrast were adjusted to visualize much brighter fluorescein-positive donor cells. Transplanted wild-type cells contribute to EB placodes in *hsp70::dn-fgfr1* embryos (arrowheads, top). Scale bars: 50 μm. o, otic placode.

excluded from them (Fig. 3A and Table 1). Moreover, we often observed that when transgenic donor cells resided within the EB placodes, they did not express Pax2 (Fig. 3A). In reciprocal experiments, wild-type cells were transplanted into *hsp70::dn-fgfr1* embryos. Resulting embryos were heat shocked at 13.5-16 hpf and analyzed for Pax2 expression at 24 hpf (Fig. 3B). The majority of transplanted wild-type cells remained dorsally, at the level of the otic vesicle; however, some migrated ventrolaterally and contributed to EB placodes (Fig. 3B). When compared with the contralateral control side, the total number of Pax2-positive cells on the transplanted side was significantly increased (54 versus 42, $P<0.004$, paired *t*-test; Fig. 3B and Table 1). If embryos were heat shocked earlier (10-13.5 hpf), wild-type cells were completely excluded from the presumptive EB placode region (data not shown). Overall, these data demonstrate a cell-autonomous requirement for Fgf signaling, consistent with our previous observations that Fgf signaling is active in the EB placodes.

Mesoderm is likely source of EB placode-inducing signal

To find a potential source of a placode-inducing signal, we analyzed *foxi1* and *pax2a* expression in mutant embryos where cephalic mesoderm and endoderm were missing (Fig. 4A). *Maternal-Zygotic one-eyed pinhead* (*MZoep*) mutants are deficient in Nodal signaling and completely lack cephalic mesoderm and endoderm, whereas gross specification of the neural tube is normal (Gritsman et al., 1999). In contrast, embryos mutant for the *sox*-related transcription factor *casanova* (*cas*) are missing endoderm (Alexander et al., 1999; Kikuchi et al., 2001). *foxi1* expression was severely reduced, whereas *pax2a* expression was absent in *MZoep* mutants, a phenotype identical to that

Table 1. Fgf signaling is required cell-autonomously in EB placodes[1]

	n[2] (total)	n[3] (target)	Total number of Pax2 cells in f[4] placode	Total number of Pax2 cells in g and v placodes	Average number of Pax2 donor cells in f placode	Average number of Pax2donor cells in g and v placodes
wt→wt	176	46 (26%)	44	70	11	13
hsp70::dn-fgfr1→wt	112	39 (35%)	39[5]	66	1[6]	3[6]
	n[2] (total)	n[3] (target)	Total number of Pax2 cells	Average number of Pax2 host cells	Average number of Pax2 donor cells	
wt→*hsp70::dn-fgfr1* (transplant side)	78	20 (26%)	54[7]	39	15	
wt→*hsp70::dn-fgfr1* (contralateral control)			42	42	0	

[1]25-30 donor cells were transplanted into the presumptive placodal domain of shield-staged host embryos (Fig. 3); resulting embryos were heat-shocked at 38.5°C for 30 minutes (bud-3s for *hsp70::dn-fgfr1*→wt transplants and 9-14s for wt→*hsp70::dn-fgfr1* transplants), collected at 24 hpf and analyzed for Pax2 expression.
[2]Total number of embryos that received transplanted cells.
[3]Number of embryos with at least one Pax2-positive donor cell.
[4]f, presumptive facial placode; g, presumptive glossopharyngeal placode; v, presumptive vagal placode.
[5]$P<0.014$, *t*-test.
[6]$P<0.001$, *t*-test.
[7]$P<0.004$, paired *t*-test.

resulting from reduction in Fgf signaling (Fig. 4A). However, *foxi1* expression was normal and *pax2a* expression only slightly altered in embryos injected with a *cas* morpholino (MO) (Fig. 4A). These results strongly suggest that mesoderm is the source of a placode-inducing signal.

These experiments and the time-course analysis described earlier suggest that the Fgf ligands responsible for EB placode induction would be expressed in cephalic mesoderm between 10 and 16.5 hpf. Both *fgf3* and *fgf8* were expressed in two bilateral stripes adjacent to the neural plate beginning at 10-11 hpf (Fig. 4B) (Reifers et al., 2000). Expression began as a narrow stripe lateral to the mid-hindbrain boundary and rhombomere 4 (r4). With time, expression extended both rostrally and caudally adjacent to r6-7. These patterns of expression were largely unchanged in *cas*-MO-injected embryos, but completely absent in *MZoep* embryos (see Fig. S3 in the supplementary material), arguing that *fgf3* and *fgf8* are expressed in mesoderm, not endoderm (Fig. 4B). Transverse sections through the 11- and 14-hour-old embryos confirmed that *fgf3* and *fgf8* were expressed in the underlying tissue and not ectoderm (Fig. 4C). Interestingly, the expansion of ectodermal *foxi1* expression closely correlated with changes in mesodermal *fgf3* and fgf8 expression (Fig. 4B). *foxi1* expression was upregulated just anterior to the otic placode between 11 and 12 hpf (Fig. 4B), and then extends posteriorly between 12 and 16 hpf (Fig. 4B). Thus, both *fgf3* and *fgf8* are expressed in the cephalic mesoderm at the right stage, suggesting their involvement in EB placode induction.

Fgf3 and Fgf8 are required for EB placode induction

To test whether Fgf3 and/or Fgf8 are required for EB placode induction, we crossed *limabsent* (*lia*)/*fgf3* mutants (Herzog et al., 2004) with *acerebellar* (*ace*); *fgf8* mutants (Reifers et al., 1998). Whereas the *fgf3* (*lia*^{t24149}) allele is null (Herzog et al., 2004), the *fgf8* (*ace*^{it282}) allele is a hypomorph that retains about 25% of Fgf8 activity (Draper et al., 2001). Resulting trans-heterozygous fish were intercrossed to generate all genotypic combinations (including *fgf3;fgf8* double mutants), which were analyzed by in-situ hybridization using PPE, EB placode and EB ganglia markers, photographed and genotyped. As expected, *pax2a* expression is lost from the isthmus in *fgf8* mutants and the otic vesicle is missing in *fgf3;fgf8* double mutants (Fig. 5A) (Leger and Brand, 2002; Liu et al., 2003; Maroon et al., 2002; Reifers et al., 1998). In addition, *fgf3* mutants lacked *ngn1* and *phox2b* expression in the glossopharyngeal and small vagal placodes and ganglia, as Fgf3 is needed for EB neurogenesis at later stages, as we previously reported (Fig. 5A) (Nechiporuk et al., 2005).

Reduction in Fgf3 and Fgf8 levels, either alone or together, did not affect formation of PPE as assessed by *eya1* and *six1* expression (Fig. 5A and data not shown). Ectodermal *foxi1* levels were strongly reduced in *fgf3;fgf8* double mutants but were not affected in either single mutant (Fig. 5A). Similarly, *pax2a*, *ngn1* and *phox2b* expression in all EB placodes and ganglia was absent or strongly reduced in *fgf3;fgf8* double mutants. We consistently observed some limited *ngn1* and *phox2a*-staining, but not *phox2b* staining, in the large vagal placode and ganglion (Fig. 5A and data not shown). Interestingly, *fgf8–/–*; *fgf3+/–* embryos displayed an intermediate phenotype between the wild type and *fgf3;fgf8* double. Because we did not observe any phenotype in *fgf8–/–* or *fgf3+/–* embryos alone, we concluded that Fgf3 and Fgf8 genetically interact.

To visualize epithelial morphology, we obtained transverse sections from wild-type and *fgf3;fgf8* double mutant embryos processed for *foxi1* and *pax2*a in situ hybridization (Fig. 5B,C). In wild type, the epithelium was well organized and displayed columnar morphology, with *foxi1* expression mostly limited to the outer ectodermal layer. In contrast, epithelium was disorganized and remaining *foxi1* expression extended to multiple cell layers in *fgf3;fgf8* double mutants (Fig. 5B,C). Altogether, these results strongly argue that Fgf3 and Fgf8 are required for EB placode induction.

Restoration of cephalic mesoderm is sufficient to rescue EB ganglia

Both *fgf3* and *fgf8* are expressed in the neural tube at the time of EB placode induction in addition to cephalic mesoderm. We therefore performed tissue transplants to test where *fgf3+8* is required. To maximize the efficiency of these experiments, we transplanted wild-type cells into embryos injected with *fgf3+8* morpholino oligonucleotides, rather than into *fgf3;fgf8* double mutants. Because endoderm-derived Fgf3 is required for later stages of EB placode neurogenesis (Nechiporuk et al., 2005), we first determined a dose of *fgf3*-MO that alone allowed normal neurogenesis, but in conjunction with *fgf8*-MO phenocopied *fgf3;fgf8* mutants (see Fig. S4 in the supplementary material).

We injected host zebrafish embryos at the one-cell stage with *fgf3+8*-MO, and wild-type donors were injected with a fluorescein-dextran lineage tracer. At early gastrula stages (30-40% epiboly), we transplanted 25-30 cells into the margin of *fgf3+8* morphants. EB

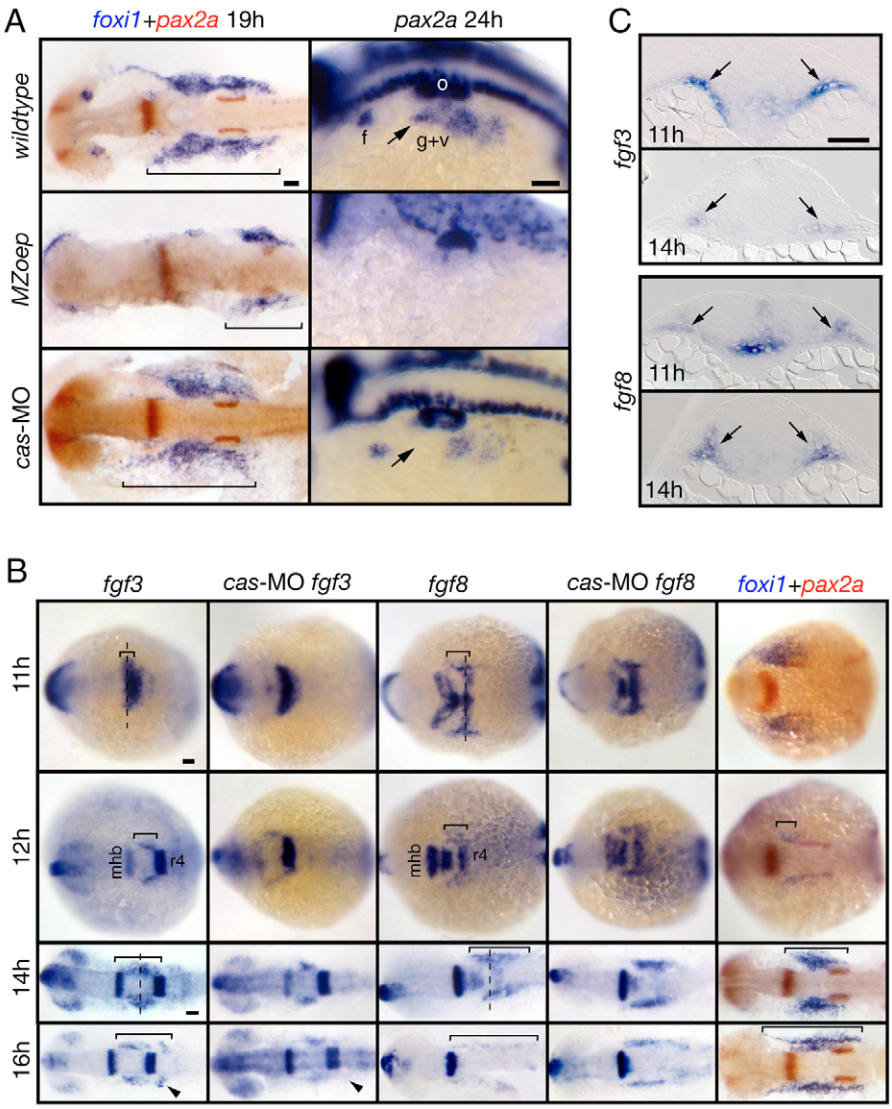

Fig. 4. Mesoderm is the likely source of the EB placode-inducing signal(s). (**A**) *MZoep* mutants and *cas* morphants were analyzed for *foxi1* and *pax2a* expression. *foxi1* panels show dorsal views, and *pax2a* panels show lateral views. *pax2a* expression was absent and *foxi1* expression was strongly reduced in *MZoep* embryos (bracket). In contrast, in *cas* morphants, *foxi1* expression was normal and *pax2a* expression was slightly reduced (arrow). (**B**) Wild-type and morphant embryos were collected at 11, 12, 14 and 16 hpf and analyzed for *fgf3*, *fgf8* and *foxi1* expression. All panels show dorsal views. The presumptive mesodermal expression of *fgf3* and *fgf8* is marked by a bracket. Note that these expression domains expand first rostrally and then caudally with time and the expression pattern is largely unchanged in *cas* morphants, with the exception of a small *fgf3*-expressing domain (arrowheads). The extent of *foxi1* expression (bracket) closely correlates with the extent of *fgf3* and *fgf8* expression. (**C**) Transverse sections (level of cross sections indicated by a dashed line in (B) revealed *fgf3* and *fgf8* expression in the mesoderm underlying ectoderm (arrows). Scale bars: 50 μm. Abbreviations are as in Fig. 1; r4, rhombomere 4.

ganglia were assessed at 54 hpf for *phox2b* mRNA expression (Fig. 6A) or at 72 hpf for *phox2b::egfp* transgene expression (Fig. 6B). The *phox2b::gfp* strain carries a stably integrated BAC clone with *egfp* recombined into the endogenous *phox2b* start site. Hindbrain transplant alone did not rescue EB ganglia (Fig. 6A and Table 2), but were capable of rescuing the Fgf requirement for locus coeruleus development (Guo et al., 1999). In contrast, mesodermal transplants alone or together with hindbrain efficiently rescued EB ganglia (Fig. 6A and Table 2). We did not observe any differences in the efficiency of the rescue between mesoderm and hindbrain transplants versus mesoderm transplants alone (Table 2). Although in some cases transplants also included pharyngeal endoderm, donor endoderm did not appear to be necessary for EB ganglia rescue in other cases (Fig. 6B; Table 2). When visualized at 72 hpf, it is apparent that donor cells contributed to the various facial muscles in the rescued embryos. From these data we conclude that the cephalic mesoderm, but not the neural tube, is sufficient to rescue EB ganglia in *fgf3+8* morphants.

Fgf3 or Fgf8 are sufficient to induce EB placodes

To test whether ectopic expression of Fgf is sufficient to induce *foxi1*-positive EB placode precursors or *phox2b*-positive EB neurons we expressed Fgf from an ectopic source. In the first series of experiments, we mosaically expressed Fgf3 or Fgf8 using heat-shock promoter constructs in wild-type embryos. Embryos were injected with *hs-fgf3myc* or co-injected with *hs-fgf8* and *hs-gfp* plasmids, heat shocked between 10 and 13 hpf, and assayed for *foxi1* expression at 19-20 hpf (Fig. 7A). As controls, we injected embryos with a *hs-gfp* plasmid alone. Injection of a plasmid results in a mosaic DNA distribution in zebrafish embryo, leading to randomly distributed *fgf*- and *gfp*-expressing clones (usually on one side of an embryo) upon heat shock. A significant number of the injected wild-type embryos exhibited ectopic *foxi1* foci, 31% (n=148) and 33% (n=228) for *hs-fgf3myc* and *hs-fgf8* injections, respectively (compare with only 4%, n=218, for *hs-gfp* alone) (Fig. 7A). Ectopic *foxi1* staining often colocalized with Myc-positive cells surrounded by punctate antibody staining, presumably recognizing secreted Myc-tagged Fgf3 (Fig. 7A).

To introduce Fgf from a more localized source, we performed bead implantation experiments. The 20-μm beads were soaked in mouse recombinant Fgf8b and placed under the ectoderm just lateral to the neural plate in wild-type embryos between 11 and 13 hpf. Resulting embryos were analyzed for *foxi1* expression at 19 hpf (Fig. 7B). Control embryos that received BSA-soaked beads showed no changes in *foxi1* expression (Table 3 and data not

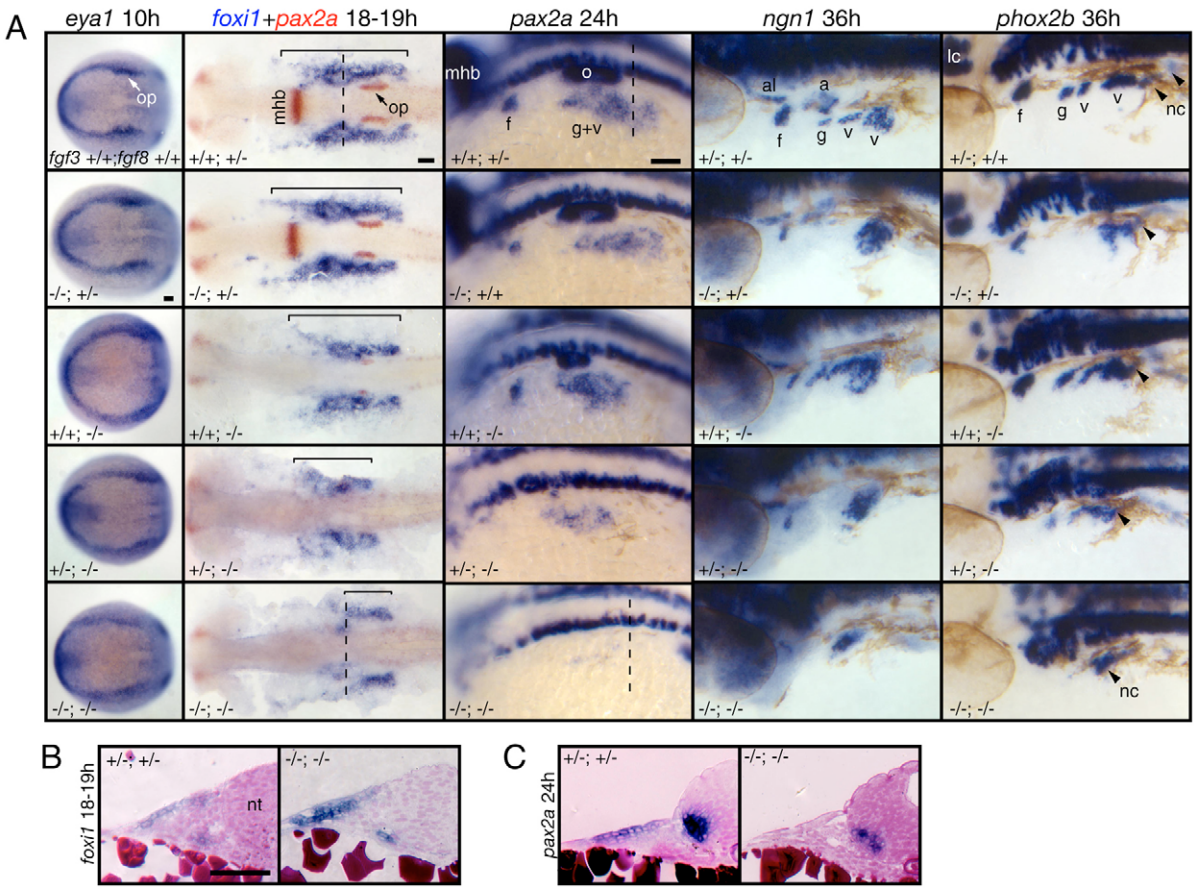

Fig. 5. Fgf3 and Fgf8 are necessary for EB placode induction. (**A**) *fgf3+/–;fgf8+/–* embryos were crossed to generate various genotypic combinations, including *fgf3;fgf8* mutants. Resulting embryos were processed for in-situ hybridization with *eya1*, *foxi1*, *pax2a*, *ngn1* and *phox2b* riboprobes, photographed and genotyped (genotypes are shown in the bottom left of each panels). All panels show lateral views, except *eya1*-expression panels, which show dorsal views. PPE is not affected in *fgf3* or *fgf8* mutants or *fgf3;fgf8* double mutant. Consistent with our previous observations (Nechiporuk et al., 2005), *fgf3* mutants lacked *ngn1* and *phox2b* expression in glossopharyngeal and small vagal ganglia, whereas *foxi1* and *pax2a* expression was normal. All markers were expressed normally in *fgf8–/–* embryos. However, *foxi1* expression (brackets) was strongly reduced and *pax2a*, *ngn1*, and *phox2b* expression was either absent or strongly reduced in *fgf3;fgf8* double mutants. Vagal neural crest is not affected in *fgf3;fgf8* double mutants (arrowheads). *fgf3+/–;fgf8–/–* embryos displayed intermediate phenotypes, where expression of all markers were reduced but not absent. (**B**,**C**) Transverse sections of *fgf3/8* double mutants and wild-type siblings were obtained from the whole-mounts processed for *foxi1* (B) and *pax2a* (C) in situ (dashed lines in A indicate level of cross section). In contrast to wild type, the epithelium appears disorganized and *foxi1* expression is not restricted to a single cell layer in *fgf3;fgf8* mutants. *pax2a* expression is absent from the ectoderm in *fgf3;fgf8* mutants. Scale bars: 50 μm. Abbreviations are as in Fig. 1; a, acoustic ganglion; al, anterior lateral line ganglion; op, otic placode.

shown). In contrast, we observed ectopic *foxi1* expression foci in the vicinity of the Fgf8b-coated beads in 40% of the analyzed embryos (n=15; Fig. 7B and Table 3). Fig. 7C summarizes the location of ectopic *foxi1* expression from all ectopic Fgf over-expression experiments. We observed ectopic foci throughout the ectoderm located ventrally to the endogenous *foxi1* expression domain, but found no ectopic foci dorsal to the endogenous domain or in trunk ectoderm.

In chick embryos, placodal precursors are initially specified as lens prior to acquiring their definitive fates, and subsequently the lens fate is restricted by Fgf8 signals derived from the anterior neural plate (Bailey et al., 2006). To determine whether anterior expansion of *foxi1* by ectopic Fgf expression similarly affects lens specification, we assayed *hs-fgf3myc*-injected embryos for a lens marker Prox1 (Tomarev et al., 1998; Wigle et al., 1999). Almost all embryos with rostral expansion of *foxi1* expression displayed either reduction or absence of lens Prox1 expression (15/17; Fig. 7D). We also observed a similar result using Fgf8b-coated beads (3/4; data not shown). This result implies that more anterior PPE can be respecified to form EB placode precursors, at the expense of lens precursors.

To confirm that the ectopically generated *foxi1*-positive precursors could give rise to EB neurons, we assayed wild-type embryos after bead implantation for *phox2b* expression at 48 hpf. Most embryos displayed ectopic *phox2b*-positive foci (6/10; Fig. 7E and Table 3). Similarly, activation of *hs-fgf3myc* or *hs-fgf8* at 12-13 hpf also resulted in formation of ectopic foci. Importantly, a number of ectopic *phox2b*-positive foci were located on the ventral side of the head and belly ectoderm, away from the endogenous *phox2b*-expression sites and pharyngeal endoderm (Fig. 7F). Analyses of *phox2b::egfp* embryos revealed that the ectopic cells extended peripheral projections, confirming their neuronal identity. When ectopic *phox2b*-positive foci were located adjacent to the eye, we often observed either reduction or complete loss of lens tissue (Fig.

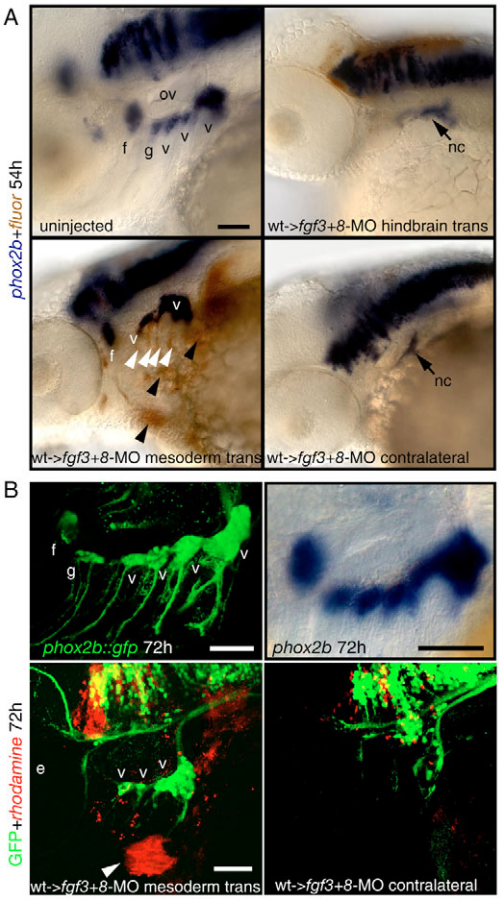

Fig. 6. Restoration of cephalic mesoderm is sufficient to rescue EB ganglia. Wild-type donor embryos were injected with a lineage tracer fluorescein (**A**, brown), or rhodamine (**B**, red). At 30-40% epiboly, 25-30 donor cells were transplanted into the margin of *fgf3+8*-MO hosts. Mosaic embryos were collected at 54 (A) or 72 (B) hpf and analyzed for *phox2b* (blue, A) or GFP expression (green, B), respectively. (A) Lateral views of an uninjected control embryo (top, left) or *fgf3+8* hosts that received hindbrain or mesodermal transplant. Note that mesodermal wild-type donor cells (brown stain, black arrowheads) efficiently rescued facial and vagal ganglia when compared with the contralateral control. Some donor cells also contributed to pharyngeal endoderm (white arrowheads). (B) *phox2b::egfp* transgene (top, left) recapitulates *phox2b* expression in the EB ganglia when compared with the endogenous message (top, right). Lateral view of the 72-hour old mosaic *phox2b::egfp* embryo that showed rescue of the vagal ganglia (compare with the contralateral side on the right). Donor cells (red, arrowhead) contributed to the facial muscles, indicating mesodermal origin. Note that in this example donor cells did not contribute to the endodermal pouches. Scale bars: 50 μm. Abbreviations are as in Fig. 1; ov, otic vesicle.

7G, top panels). We confirmed that formation of ectopic *phox2b*-positive neurons did not require the presence of endodermal pouch tissue, as assayed by an endodermal pouch marker *nkx2.3* (Lee et al., 1996). This result is consistent with previous observations demonstrating that a subset of EB placodal cells did not require endoderm-derived signals to undergo neurogenesis (Holzschuh et al., 2005; Nechiporuk et al., 2005). Overall our data show that Fgf-induced ectopic *foxi1*-positive precursors could differentiate into *phox2b*-positive epibranchial neurons.

Table 2. Cephalic mesoderm restoration in *fgf3;fgf8* morphants rescues EB ganglia[1]

wt→*fgf3+8*-MO	n[2]	gVII[3]	gIX	Small gX	Large gX
Mesoderm alone	8	3	1	3	8
Mesoderm and hindbrain	7	1	2	2	6
Hindbrain alone	42	0	0	0	0
Total rescued	15	4 (1[4])	3 (2)	5 (2)	14 (4)

[1]25-30 donor cells were transplanted into the margin of a host embryo at 30-40% epiboly (Fig. 6); resulting embryos were collected at either 48 or 72 hpf and analyzed for *phox2b* (wild-type hosts) or EGFP (*phox2b::egfp* hosts) expression, respectively.
[2]Out of 226 embryos that received the transplant, 15 (7%) displayed rescue of at least one EB ganglion.

To determine whether Fgf is sufficient to restore *foxi1* expression in Fgf-deficient embryos, we also injected *hs-fgf3myc* and *hs-fgf8* plasmids into *fgf3+8* morphants. Either construct efficiently restored the extent of the endogenous *foxi1* expression domain (Fig. 8A). A total of 33% of *hs-fgf3myc* injected embryos (*n*=161) and 20% of *hs-fgf8*-injected embryos (*n*=135) had one side of *foxi1* expression domain restored when compared with the contralateral control. Moreover, induction of Fgf3 at the 10 hpf stage restored EB ganglia in 27% (*n*=72) of embryos (compare with 6% in *fgf3+8*-MO, *n*=80) (Fig. 8B). We also performed bead implantation experiments in *fgf3+8* morphants. When beads were placed in the tissue lateral to the neural plate we observed restoration of the *foxi1* expression domain (12/15; Fig. 8C and Table 3). We often observed *foxi1* expression a few cell diameters away from the bead, suggesting that Fgf acts over a distance. In contrast, we did not observe rescue of *foxi1* expression when beads were placed in the hindbrain (0/5; Table 3). These results are consistent with our previous finding that a hindbrain source is not sufficient as an Fgf-inducing signal.

DISCUSSION

Taken together, our data demonstrate a requirement for mesodermally-derived *fgf3* and *fgf8* for generation of EB placodes. We propose that a subset of cells within the PPE are induced by Fgf signaling to form a *foxi1* expression domain, and it is from within this domain that *pax2a*+ EB placodes are derived. Once a *foxi1*-positive field of precursors is established, *pax2a* expression appears in an anterior-to-posterior sequence: first, in the facial placode at 16-18 hpf and then in the glossopharyngeal and vagal placodes at 18-22 hpf. Expression of *pax2a* is more restricted than that of *foxi1* and *pax2a* is never expressed in the *foxi1*-positive ectoderm between facial and glossopharyngeal placodes, a region that is devoid of neurogenesis. Thus, *pax2a* expression within this *foxi1*-positive field of precursors might indicate the commitment of these cells to neurogenic EB placode fate. Further studies will be necessary to test this hypothesis.

Although mesodermal Fgf signals are necessary for both the expansion of *foxi1* and the induction of *pax2a*, our analysis suggests that the critical event is the establishment of *foxi1* expression. The timing of expansion of *foxi1* expression to include the presumptive EB placode domain corresponds to the anterior and posterior spread of *fgf3* and *fgf8* expression in cranial mesoderm between 10 and 14 hpf, precisely the critical period delineated by inhibitor studies and, significantly, before the initiation of *pax2a* expression at 16 hpf. Interestingly, *pax2a* has been similarly suggested to act downstream of Fgf and Foxi1 signals in otic placode formation (Hans et al., 2004).

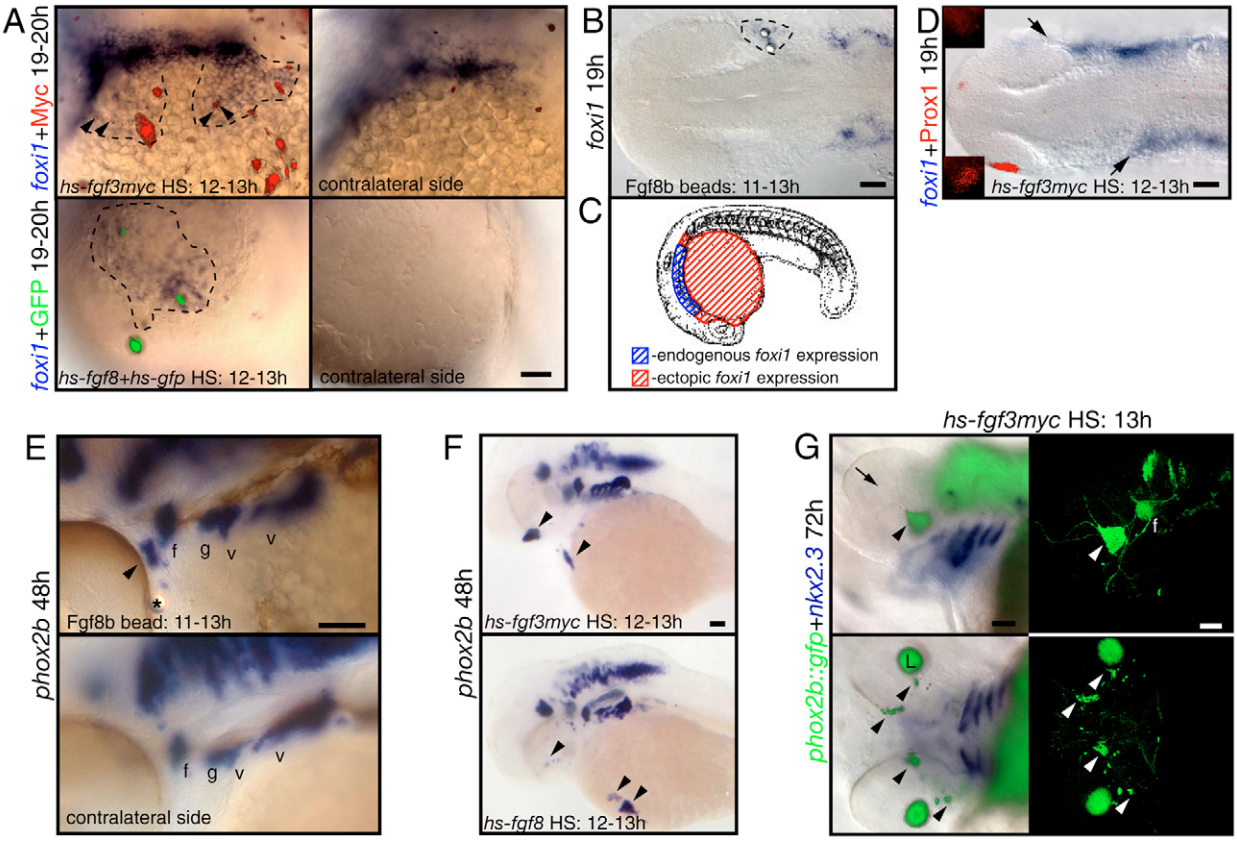

Fig. 7. Fgf3 or Fgf8 is sufficient to induce *foxi1*-positive EB precursors and *phox2b*-positive EB neurons in wild-type embryos. Zebrafish embryos were injected with *hs-fgf3myc* or coinjected with *hs-fgf8* and *hs-gfp* plasmids at one-cell stage, heat shocked at 10-13 hpf and then assayed for *foxi1* or *phox2b* expression (blue). Alternatively, embryos were implanted with Fgf8b-coated beads at 11 hpf and assayed for *foxi1* and *phox2b* expression at 19 and 48 hpf, respectively. (A,E,F) Lateral views; (B,D) dorsal views. (**A**) Ectopic *foxi1*-positive cells (outlined by dotted line) are immediately adjacent to the Myc- (red) or GFP-positive (green) cells expressing Fgf. Note punctate staining surrounding Myc-positive cells, presumably indicating secreted myc-tagged Fgf3 protein. (**B**) Ectopic *foxi1* expression (dotted line) was induced in the vicinity of Fgf8b beads. (**C**) Summary of the ectopic Fgf expression experiments. Ectopic *foxi1* foci (shown in red) were restricted to the ventral side of the yolk surface, just ventral and anterior to the endogenous *foxi1*-expression domain. (**D**) Activation of *hs-fgf3myc* leads to the anterior expansion of *foxi1* domain (arrows) and loss of Prox1 expression in the lens (red). Insets show lateral views of the presumptive lens domain on each side of the embryo. (**E**) Fgf8b bead (star) induced formation of the ectopic *phox2b*-positive EB neurons (arrowhead). (**F**,**G**) Activation of Fgf3myc or Fgf8 in wild-type (F) or *phox2b::egfp* transgenic embryos (G) induced ectopic *phox2b*-positive EB neurons (arrowheads) away from the endogenous *phox2b*-expression sites. (G) Left panels show overlay of immunofluorescence and brightfield photographs, and right panels show confocal stacks generated from the same embryos. Note ectopic *phox2b*-positive cells on the ventral surface of the head as well as in the eye (arrowheads). Formation of the ectopic *phox2b*-positive neurons (green) did not require endoderm pouch tissue, visualized by *nkx2.3* (purple). Note complete absence of lens tissue (arrow,

What is the role of Pax2a in the EB placode development? Targeted inactivation of mouse Pax2 demonstrated that it is required for ear patterning and acoustic ganglion development (Burton et al., 2004; Torres et al., 1996), but its function in EB placode development was not determined. Pax2 expression has been described in EB placodes in chick and *Xenopus* (Baker and Bronner-Fraser, 2000; Schlosser and Ahrens, 2004), but not previously in zebrafish. We found that, in zebrafish *pax2a* mutants, the development of some but not all EB neurons was disrupted. It is possible that other *pax* genes may play redundant roles during EB placode development, similar to the situation for the otic placode. Whereas *pax2a* mutants have a very mild reduction of the otic placode, injection of *pax8* morpholino results in its almost complete absence (Hans et al., 2004; Mackereth et al., 2005). Interestingly, *pax8* expression has been reported in the EB placode in *Xenopus* (Schlosser and Ahrens, 2004). Pax2b, a zebrafish ortholog of Pax2a (Pfeffer et al., 1998), may also play a redundant role during EB placode development.

Model of EB placode induction in zebrafish

To summarize data presented here and by others, we suggest the following model for EB placode induction (Fig. 9). Bmp, Wnt and Fgf signals are responsible for the initial specification and positioning of the PPE domain (Ahrens and Schlosser, 2005; Brugmann et al., 2004; Litsiou et al., 2005). After the PPE is formed, the ventral part of the competent ectoderm receives Fgf3 and Fgf8 signals from the cephalic mesoderm (Fig. 9A). Importantly, Fgf signals are not required for the initial induction of *foxi1* expression, as *foxi1* message is still present in Fgf-deficient embryos. Residual *foxi1* expression may represent a subset of cells that will not

Table 3. Fgf8 over-expression is sufficient to induce *foxi1*-positive EB precursors and *phox2b*-positive EB neurons[1]

Bead→host	Stage (hpf)/ marker[2]	n[3]	Ectopic/ rescued
BSA→wt	19/*foxi1*	9	0
Fgf8b→wt	19/*foxi1*	15	6
BSA→wt	48/*phox2b*	12	0
Fgf8b→wt	48/*phox2b*	10	6
BSA→*fgf3+8*-MO	19/*foxi1*	11	0
Fgf8b→*fgf3+8*-MO	19/*foxi1*	15	12
Fgf8b→*fgf3+8*-MO (hindbrain)	19/*foxi1*	5	0

[1]One to three BSA- or Fgf8b-coated beads were implanted into wild-type or *fgf3;fgf8* morphants at 11-13 hpf (Fig. 7).
[2]Resulting embryos were collected at either 19 or 48 hpf and analyzed for *foxi1* or

normally contribute to EB placodes, or may indicate cells that are stalled in the early stages of their development. Although our misexpression experiments demonstrated that most of the PPE and ventral embryonic ectoderm are competent to express *foxi1*, only the ventral portion of the PPE normally expresses it. While the *foxi1* expression domain remains broad, *pax2a* expression is refined over the course of development: *pax2a* is more restricted than *foxi1* and is expressed only in the individual placodes during neurogenesis. Our observations support a multi-step model of EB placode induction where a first step is to induce a broad field of precursors marked by *foxi1* expression, which is further refined by other signals

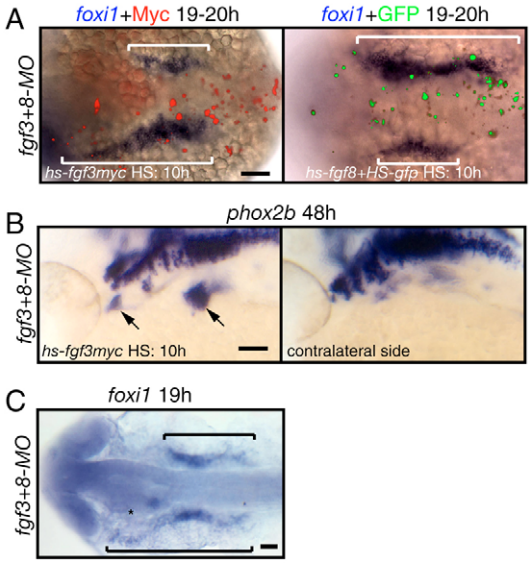

Fig. 8. Fgf3 or Fgf8 is sufficient to induce *foxi1*-positive EB precursors and *phox2b*-positive EB neurons in *fgf3+8* morphants. (A,C) Dorsal views; (B) lateral views. (**A**,**B**) Zebrafish embryos were injected with *hs-fgf3myc* or co-injected with *hs-fgf8* and *hs-gfp* plasmids at one-cell stage, heat shocked at 10-13 hpf and then assayed for *foxi1*or *phox2b* expression (blue) and Myc or GFP expression (red and green, respectively). Fgf3myc or Fgf8 efficiently rescued *foxi1* (brackets in A) or *phox2b* (arrows in B) expression in *fgf3+8* morphants. Note the difference between *foxi1* expression domain adjacent to Myc or GPF-expressing cells and contralateral side. (**C**) *fgf3+8* morphant

during later steps of development. This multi-step model might explain how otic and EB precursors interpret the same Fgf signals. Close proximity of cephalic mesoderm to the ventral part of competent ectoderm might help to restrict *foxi1*+ EB precursors. Alternatively, additional signal(s), possibly from a different source, might distinguish EB and otic precursors. In support of this idea, a recent study demonstrated that in addition to inductive Fgf signals, Wnt signals, possibly from hindbrain, help refine otic placode positioning in mouse embryos (Ohyama et al., 2006).

In addition to their roles in EB placode induction, Fgf3 and Fgf8 derived from the cephalic mesoderm and neural tube pattern the pharyngeal pouches (Fig. 9A) (Crump et al., 2004). We suggest dual roles for Fgf3 and Fgf8 in the initial development of these tissues to ensure the subsequent developmental coordination of EB neurons and their target of innervation. Signals from pharyngeal pouch endoderm, including *fgf3*, *bmp2b* and *bmp5,* are required to initiate expression of the early proneural genes such as *ngn1* and *neuroD* (*nrd*) in the individual EB placodes (Fig. 9B) (Holzschuh et al., 2005; Nechiporuk et al., 2005). *ngn1* is also transiently expressed in migrating and condensing neuroblasts, and is required for the subsequent formation of *phox2*-positive neuronal precursors (Andermann et al., 2002; Nechiporuk et al., 2005). Eventually, *phox2*-positive precursors condense together with neural-crest-derived glia to form cranial ganglia. Further studies will be necessary to determine what cues guide EB neurons to their final destination**.**

It has been suggested previously that pharyngeal endoderm is required for EB placode induction in avian embryos (Begbie et al., 1999). Therefore, one might interpret our results showing a role for mesodermal Fgf signaling in zebrafish placode induction as simply a reflection of the Fgf requirement for pharyngeal pouch development (Crump et al., 2004). However, there are several arguments against this explanation. First, in zebrafish, pharyngeal pouches do not begin to form until 22 hpf (Holzschuh et al., 2005), well after *pax2a* expression is established in the thickened EB ectoderm (this study). Second, loss of pharyngeal endoderm in zebrafish *casanova* mutants results not in elimination of EB placodes but rather reduction in neurogenesis; expression of *ngn1*, *phox2b* and the Hu antigen is lost, whereas *foxi1*, *pax2a* and morphological thickening of the ectoderm is retained (Holzschuh et al., 2005; Nechiporuk et al., 2005) (this study). Although this result may reflect differences between fish and avian species, it is

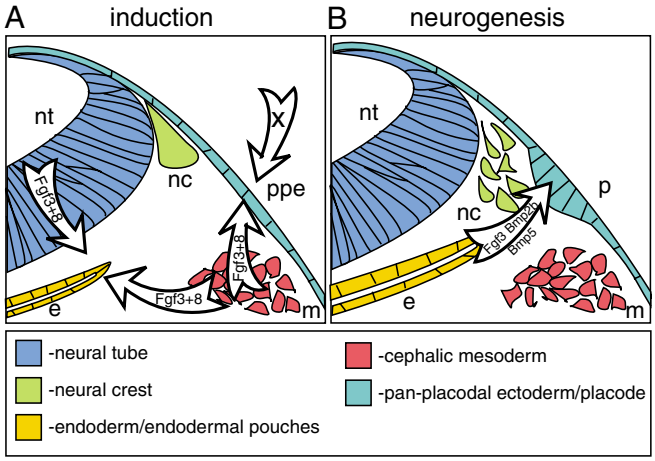

Fig. 9. A model of EB placode induction in zebrafish. See text for details.

important to note that only late markers of neurogenesis (Phox2a, NF-M) were analyzed in the previous avian study (Begbie et al., 1999), leaving open the possibility that mechanisms might be conserved. Third, our mosaic analysis demonstrates that Fgf signaling is required directly within the ectoderm, suggesting that the mesodermal Fgf signal is received directly by placodal precursors. Finally, we show that ectopic expression of Fgf results in formation of new *phox2b*-positive neurons in the absence of *nkx2.3*+ pharyngeal endoderm. Although we cannot rule out that pharyngeal endoderm supplies additional EB-promoting signals, our results strongly support a role for mesodermal Fgf directly acting upon placodal ectoderm.

Role of Fgf signaling in specification and induction of EB placodes

FGFs play a critical role in morphogenesis of multiple organ systems by regulating cell proliferation, differentiation, cell migration and cell survival. Thus, Fgf signals could regulate expansion of *foxi1*-positive precursors by any of the above mechanisms. Fgf signals can act as chemoattractants during both invertebrate and vertebrate development. In *Drosophila*, Fgf plays the role of a chemotactic signal during tracheal morphogenesis (Sutherland et al., 1996), whereas in worms, the Fgf signal guides sex myoblasts to the gonads (Burdine et al., 1998; Burdine et al., 1997). Fgf4 and Fgf8 act as chemotactic signals to directly coordinate cell movements during gastrulation in the chick embryo (Yang et al., 2002). We observed that *foxi1* expression could be induced a few cell diameters away from an Fgf source, arguing that Fgf might function as a long-range signal to recruit EB placode precursors. This is consistent with recent work in zebrafish revealing that Fgf ligand could travel as far as 16-cell diameters away from an Fgf source (Scholpp and Brand, 2004). Although it is attractive to speculate that Fgf signals could promote migration, further studies are necessary to define the exact role of Fgf3 and Fgf8 in the recruitment of EB placode precursors.

Conservation of the inductive signals in the cranial placodes

It has been argued that once the PPE domain is established, local signal(s) promote the fate of the individual placodes (Streit, 2004). The initial step common to all placodes include signals from mesendoderm (Ahrens and Schlosser, 2005; Litsiou et al., 2005), whereas later inductive signals for specific placodes would originate from distinct tissues. Dorsolateral (trigeminal, lateral line and otic) placodes are in close proximity to the neural tube, whereas ventrolateral (EB) placodes are in close contact with the endoderm and cephalic mesoderm. Indeed, Fgf signals from the neural tube are required during otic placode development (Leger and Brand, 2002), and neural tube signal(s) is sufficient to induce trigeminal placode markers in the head ectoderm, although the nature of this signal(s) is still unknown (Stark et al., 1997).

There are surprising similarities between otic and EB placode development. Both otic and EB placodes require *eya1* and *six1* (Ozaki et al., 2004; Xu et al., 1999; Xu et al., 2003; Zheng et al., 2003; Zou et al., 2004), and their precursors are intermingled in the PPE (Streit, 2002). Mesodermal Fgfs are involved in the initial induction of each placode from PPE (Kil et al., 2005; Wright and Mansour, 2003), and induction is regulated by *foxi1* to induce expression of *pax2a* (Mackereth et al., 2005; Nissen et al., 2003; Solomon et al., 2003; Solomon et al., 2004). Finally, Fgf signals subsequently regulate neurogenesis from both EB and otic placodes upstream of *ngn1* (Alsina et al., 2004; Nechiporuk et al., 2005). Although it is not surprising that the six/eya/dach network is conserved in various ectodermal placodes, as these transcription factors are expressed during PPE formation and are important for PPE development, it is remarkable that the same Fgf inductive signals are conserved in the EB and otic placodes.

However, it is important to note that although Fgf3 and Fgf8 signals are necessary during both otic and EB placode induction, we were able to separate the timing and Fgf requirement during these two processes. First, we defined a separate time-window requirement for Fgf signaling during EB placode development. During the otic placode induction, Fgf signaling is not required beyond 11 hpf, whereas it is essential until 16.5 hpf during EB placode development. Second, ectopic activation of Fgf signaling at 13 hpf, well after the otic placodes had been induced, promotes formation of the *foxi1*-positive precursors and EB-specific *phox2b*-positive neurons. Finally, analyses of *MZoep* mutants, which completely lack EB placodes while their otic vesicles are only reduced, support the idea that Fgf signaling plays distinct roles during initial stages of the otic and EB placode development. Alternatively, because EB and otic precursors are initially intermingled within PPE (Schlosser and Ahrens, 2004; Streit, 2002), it is possible that the same signals, including Fgfs, might control initial specification of common precursors. Interestingly, inhibition of Fgf signaling during gastrulation in zebrafish blocks expression of the early otic placode markers (Maroon et al., 2002; Phillips et al., 2001). It will be interesting to investigate whether this early Fgf block affects EB placode development as well.

The preservation of the molecular cascades involved in each type of placode development might be even more conserved than had previously been anticipated. A recent report suggests that Fgfs promote olfactory placode at the expense of lens, the ground state for cranial placodes (Bailey et al., 2006); we found similarly that Fgfs promote formation of *foxi1*+ placode precursors while simultaneously blocking lens formation. Fgfs are also involved in neurogenesis from olfactory epithelium (DeHamer et al., 1994; Kawauchi et al., 2005), suggesting that recurrent roles for Fgfs are also a common theme in placode formation. Surprisingly, Fgf signaling is also important during inductive phases of the lens placode, although the identity of Fgf ligands involved remains unknown (Faber et al., 2001). Overall, our findings are consistent with the idea that new placodes have arisen by co-option of similar molecular mechanisms, while the tissue origin of the inducing signal diverged over the course of evolution.

We thank B. Draper for sharing reagents and L. Maves for *hs-fgf3myc* construct. We are grateful to A. Fritz and R. Esterberg for providing *foxi1* mutants, M. Hammerschmidt and W. Herzog for *fgf3* mutants, G. Weidinger and C. Thorpe for *pax2a* mutants, and D. Szeto for *MZoep* mutants. We are grateful to D. Kimelman for critical comments on the manuscript. We thank D. White for excellent fish care. A.N. is supported by NRSA postdoctoral fellowship from the NICHD. Research was supported by grants to D.W.R. from NIH.

Supplementary material

Supplementary material for this article is available at
http://dev.biologists.org/cgi/content/full/134/3/611/DC1

References

Ahrens, K. and Schlosser, G. (2005). Tissues and signals involved in the induction of placodal Six1 expression in Xenopus laevis. *Dev. Biol.* **288**, 40-59.

Alexander, J., Rothenberg, M., Henry, G. L. and Stainier, D. Y. (1999). casanova plays an early and essential role in endoderm formation in zebrafish. *Dev. Biol.* **215**, 343-357.

Alsina, B., Abello, G., Ulloa, E., Henrique, D., Pujades, C. and Giraldez, F. (2004). FGF signaling is required for determination of otic neuroblasts in the chick embryo. *Dev. Biol.* **267**, 119-134.

Andermann, P., Ungos, J. and Raible, D. W. (2002). Neurogenin1 defines zebrafish cranial sensory ganglia precursors. *Dev. Biol.* **251**, 45-58.

Bailey, A. P., Bhattacharyya, S., Bronner-Fraser, M. and Streit, A. (2006). Lens specification is the ground state of all sensory placodes, from which FGF promotes olfactory identity. *Dev. Cell* **11**, 505-517.
Baker, C. V. and Bronner-Fraser, M. (2000). Establishing neuronal identity in vertebrate neurogenic placodes. *Development* **127**, 3045-3056.
Begbie, J., Brunet, J. F., Rubenstein, J. L. and Graham, A. (1999). Induction of the epibranchial placodes. *Development* **126**, 895-902.
Bessarab, D. A., Chong, S. W. and Korzh, V. (2004). Expression of zebrafish six1 during sensory organ development and myogenesis. *Dev. Dyn.* **230**, 781-786.
Brugmann, S. A., Pandur, P. D., Kenyon, K. L., Pignoni, F. and Moody, S. A. (2004). Six1 promotes a placodal fate within the lateral neurogenic ectoderm by functioning as both a transcriptional activator and repressor. *Development* **131**, 5871-5881.
Burdine, R. D., Chen, E. B., Kwok, S. F. and Stern, M. J. (1997). egl-17 encodes an invertebrate fibroblast growth factor family member required specifically for sex myoblast migration in Caenorhabditis elegans. *Proc. Natl. Acad. Sci. USA* **94**, 2433-2437.
Burdine, R. D., Branda, C. S. and Stern, M. J. (1998). EGL-17(FGF) expression coordinates the attraction of the migrating sex myoblasts with vulval induction in C. elegans. *Development* **125**, 1083-1093.
Burton, Q., Cole, L. K., Mulheisen, M., Chang, W. and Wu, D. K. (2004). The role of Pax2 in mouse inner ear development. *Dev. Biol.* **272**, 161-175.
Crump, J. G., Maves, L., Lawson, N. D., Weinstein, B. M. and Kimmel, C. B. (2004). An essential role for Fgfs in endodermal pouch formation influences later craniofacial skeletal patterning. *Development* **131**, 5703-5716.
Dauger, S., Pattyn, A., Lofaso, F., Gaultier, C., Goridis, C., Gallego, J. and Brunet, J. F. (2003). Phox2b controls the development of peripheral chemoreceptors and afferent visceral pathways. *Development* **130**, 6635-6642.
DeHamer, M. K., Guevara, J. L., Hannon, K., Olwin, B. B. and Calof, A. L. (1994). Genesis of olfactory receptor neurons in vitro: regulation of progenitor cell divisions by fibroblast growth factors. *Neuron* **13**, 1083-1097.
Draper, B. W., Morcos, P. A. and Kimmel, C. B. (2001). Inhibition of zebrafish fgf8 pre-mRNA splicing with morpholino oligos: a quantifiable method for gene knockdown. *Genesis* **30**, 154-156.
Faber, S. C., Dimanlig, P., Makarenkova, H. P., Shirke, S., Ko, K. and Lang, R. A. (2001). Fgf receptor signaling plays a role in lens induction. *Development* **128**, 4425-4438.
Fode, C., Gradwohl, G., Morin, X., Dierich, A., LeMeur, M., Goridis, C. and Guillemot, F. (1998). The bHLH protein NEUROGENIN 2 is a determination factor for epibranchial placode-derived sensory neurons. *Neuron* **20**, 483-494.
Gritsman, K., Zhang, J., Cheng, S., Heckscher, E., Talbot, W. S. and Schier, A. F. (1999). The EGF-CFC protein one-eyed pinhead is essential for nodal signaling. *Cell* **97**, 121-132.
Guo, S., Brush, J., Teraoka, H., Goddard, A., Wilson, S. W., Mullins, M. C. and Rosenthal, A. (1999). Development of noradrenergic neurons in the zebrafish hindbrain requires BMP, FGF8, and the homeodomain protein soulless/Phox2a. *Neuron* **24**, 555-566.
Hans, S., Liu, D. and Westerfield, M. (2004). Pax8 and Pax2a function synergistically in otic specification, downstream of the Foxi1 and Dlx3b transcription factors. *Development* **131**, 5091-5102.
Herzog, W., Sonntag, C., von der Hardt, S., Roehl, H. H., Varga, Z. M. and Hammerschmidt, M. (2004). Fgf3 signaling from the ventral diencephalon is required for early specification and subsequent survival of the zebrafish adenohypophysis. *Development* **131**, 3681-3692.
Holzschuh, J., Wada, N., Wada, C., Schaffer, A., Javidan, Y., Tallafuss, A., Bally-Cuif, L. and Schilling, T. F. (2005). Requirements for endoderm and BMP signaling in sensory neurogenesis in zebrafish. *Development* **132**, 3731-3742.
Jacobson, A. G. (1963). The determination and positioning of the nose, lens, and ear. III. Effects of reversing the anterior-posterior axis of epidermis, neural plate and neural fold. *J. Exp. Zool.* **154**, 293-303.
Kawauchi, S., Shou, J., Santos, R., Hebert, J. M., McConnell, S. K., Mason, I. and Calof, A. L. (2005). Fgf8 expression defines a morphogenetic center required for olfactory neurogenesis and nasal cavity development in the mouse. *Development* **132**, 5211-5223.
Kiefer, P., Strahle, U. and Dickson, C. (1996). The zebrafish Fgf-3 gene: cDNA sequence, transcript structure and genomic organization. *Gene* **168**, 211-215.
Kikuchi, Y., Agathon, A., Alexander, J., Thisse, C., Waldron, S., Yelon, D., Thisse, B. and Stainier, D. Y. (2001). casanova encodes a novel Sox-related protein necessary and sufficient for early endoderm formation in zebrafish. *Genes Dev.* **15**, 1493-1505.
Kil, S. H., Streit, A., Brown, S. T., Agrawal, N., Collazo, A., Zile, M. H. and Groves, A. K. (2005). Distinct roles for hindbrain and paraxial mesoderm in the induction and patterning of the inner ear revealed by a study of vitamin-A-deficient quail. *Dev. Biol.* **285**, 252-271.
Kimmel, C. B., Ballard, W. W., Kimmel, S. R., Ullmann, B. and Schilling, T. F. (1995). Stages of embryonic development of the zebrafish. *Dev. Dyn.* **203**, 253-310.
Korzh, V., Sleptsova, I., Liao, J., He, J. and Gong, Z. (1998). Expression of zebrafish bHLH genes ngn1 and nrd defines distinct stages of neural differentiation. *Dev. Dyn.* **213**, 92-104.
Kozlowski, D. J., Murakami, T., Ho, R. K. and Weinberg, E. S. (1997). Regional cell movement and tissue patterning in the zebrafish embryo revealed by fate mapping with caged fluorescein. *Biochem. Cell Biol.* **75**, 551-562.
Krauss, S., Johansen, T., Korzh, V. and Fjose, A. (1991). Expression of the zebrafish paired box gene pax[zf-b] during early neurogenesis. *Development* **113**, 1193-1206.
Ladher, R. K., Wright, T. J., Moon, A. M., Mansour, S. L. and Schoenwolf, G. C. (2005). FGF8 initiates inner ear induction in chick and mouse. *Genes Dev.* **19**, 603-613.
Lee, K. H., Xu, Q. and Breitbart, R. E. (1996). A new tinman-related gene, nkx2.7, anticipates the expression of nkx2.5 and nkx2.3 in zebrafish heart and pharyngeal endoderm. *Dev. Biol.* **180**, 722-731.
Lee, S. A., Shen, E. L., Fiser, A., Sali, A. and Guo, S. (2003). The zebrafish forkhead transcription factor Foxi1 specifies epibranchial placode-derived sensory neurons. *Development* **130**, 2669-2679.
Lee, Y., Grill, S., Sanchez, A., Murphy-Ryan, M. and Poss, K. D. (2005). Fgf signaling instructs position-dependent growth rate during zebrafish fin regeneration. *Development* **132**, 5173-5183.
Leger, S. and Brand, M. (2002). Fgf8 and Fgf3 are required for zebrafish ear placode induction, maintenance and inner ear patterning. *Mech. Dev.* **119**, 91-108.
Litsiou, A., Hanson, S. and Streit, A. (2005). A balance of FGF, BMP and WNT signalling positions the future placode territory in the head. *Development* **132**, 4051-4062.
Liu, D., Chu, H., Maves, L., Yan, Y. L., Morcos, P. A., Postlethwait, J. H. and Westerfield, M. (2003). Fgf3 and Fgf8 dependent and independent transcription factors are required for otic placode specification. *Development* **130**, 2213-2224.
Lun, K. and Brand, M. (1998). A series of no isthmus (noi) alleles of the zebrafish pax2.1 gene reveals multiple signaling events in development of the midbrain-hindbrain boundary. *Development* **125**, 3049-3062.
Mackereth, M. D., Kwak, S. J., Fritz, A. and Riley, B. B. (2005). Zebrafish pax8 is required for otic placode induction and plays a redundant role with Pax2 genes in the maintenance of the otic placode. *Development* **132**, 371-382.
Maroon, H., Walshe, J., Mahmood, R., Kiefer, P., Dickson, C. and Mason, I. (2002). Fgf3 and Fgf8 are required together for formation of the otic placode and vesicle. *Development* **129**, 2099-2108.
Martin, K. and Groves, A. K. (2006). Competence of cranial ectoderm to respond to Fgf signaling suggests a two-step model of otic placode induction. *Development* **133**, 877-887.
Maves, L., Jackman, W. and Kimmel, C. B. (2002). FGF3 and FGF8 mediate a rhombomere 4 signaling activity in the zebrafish hindbrain. *Development* **129**, 3825-3837.
Mohammadi, M., McMahon, G., Sun, L., Tang, C., Hirth, P., Yeh, B. K., Hubbard, S. R. and Schlessinger, J. (1997). Structures of the tyrosine kinase domain of fibroblast growth factor receptor in complex with inhibitors. *Science* **276**, 955-960.
Nechiporuk, A., Linbo, T. and Raible, D. W. (2005). Endoderm-derived Fgf3 is necessary and sufficient for inducing neurogenesis in the epibranchial placodes in zebrafish. *Development* **132**, 3717-3730.
Nissen, R. M., Yan, J., Amsterdam, A., Hopkins, N. and Burgess, S. M. (2003). Zebrafish foxi one modulates cellular responses to Fgf signaling required for the integrity of ear and jaw patterning. *Development* **130**, 2543-2554.
Ohyama, T., Mohamed, O. A., Taketo, M. M., Dufort, D. and Groves, A. K. (2006). Wnt signals mediate a fate decision between otic placode and epidermis. *Development* **133**, 865-875.
Ozaki, H., Nakamura, K., Funahashi, J., Ikeda, K., Yamada, G., Tokano, H., Okamura, H. O., Kitamura, K., Muto, S., Kotaki, H. et al. (2004). Six1 controls patterning of the mouse otic vesicle. *Development* **131**, 551-562.
Pandur, P. D. and Moody, S. A. (2000). Xenopus Six1 gene is expressed in neurogenic cranial placodes and maintained in the differentiating lateral lines. *Mech. Dev.* **96**, 253-257.
Pfeffer, P. L., Gerster, T., Lun, K., Brand, M. and Busslinger, M. (1998). Characterization of three novel members of the zebrafish Pax2/5/8 family: dependency of Pax5 and Pax8 expression on the Pax2.1 (noi) function. *Development* **125**, 3063-3074.
Phillips, B. T., Bolding, K. and Riley, B. B. (2001). Zebrafish fgf3 and fgf8 encode redundant functions required for otic placode induction. *Dev. Biol.* **235**, 351-365.
Raible, F. and Brand, M. (2001). Tight transcriptional control of the ETS domain factors Erm and Pea3 by Fgf signaling during early zebrafish development. *Mech. Dev.* **107**, 105-117.
Reifers, F., Bohli, H., Walsh, E. C., Crossley, P. H., Stainier, D. Y. and Brand, M. (1998). Fgf8 is mutated in zebrafish acerebellar (ace) mutants and is required for maintenance of midbrain-hindbrain boundary development and somitogenesis. *Development* **125**, 2381-2395.
Reifers, F., Walsh, E. C., Leger, S., Stainier, D. Y. and Brand, M. (2000). Induction and differentiation of the zebrafish heart requires fibroblast growth factor 8 (fgf8/acerebellar). *Development* **127**, 225-235.
Roehl, H. and Nusslein-Volhard, C. (2001). Zebrafish pea3 and erm are general targets of FGF8 signaling. *Curr. Biol.* **11**, 503-507.

Sahly, I., Andermann, P. and Petit, C. (1999). The zebrafish eya1 gene and its expression pattern during embryogenesis. *Dev. Genes Evol.* **209**, 399-410.
Sakaguchi, T., Kuroiwa, A. and Takeda, H. (2001). A novel sox gene, 226D7, acts downstream of Nodal signaling to specify endoderm precursors in zebrafish. *Mech. Dev.* **107**, 25-38.
Schlosser, G. and Ahrens, K. (2004). Molecular anatomy of placode development in Xenopus laevis. *Dev. Biol.* **271**, 439-466.
Scholpp, S. and Brand, M. (2004). Endocytosis controls spreading and effective signaling range of Fgf8 protein. *Curr. Biol.* **14**, 1834-1841.
Scholpp, S., Groth, C., Lohs, C., Lardelli, M. and Brand, M. (2004). Zebrafish fgfr1 is a member of the fgf8 synexpression group and is required for fgf8 signalling at the midbrain-hindbrain boundary. *Dev. Genes Evol.* **214**, 285-295.
Shepherd, I. T., Pietsch, J., Elworthy, S., Kelsh, R. N. and Raible, D. W. (2004). Roles for GFRalpha1 receptors in zebrafish enteric nervous system development. *Development* **131**, 241-249.
Solomon, K. S., Kudoh, T., Dawid, I. B. and Fritz, A. (2003). Zebrafish foxi1 mediates otic placode formation and jaw development. *Development* **130**, 929-940.
Solomon, K. S., Kwak, S. J. and Fritz, A. (2004). Genetic interactions underlying otic placode induction and formation. *Dev. Dyn.* **230**, 419-433.
Stark, M. R., Sechrist, J., Bronner-Fraser, M. and Marcelle, C. (1997). Neural tube-ectoderm interactions are required for trigeminal placode formation. *Development* **124**, 4287-4295.
Streit, A. (2002). Extensive cell movements accompany formation of the otic placode. *Dev. Biol.* **249**, 237-254.
Streit, A. (2004). Early development of the cranial sensory nervous system: from a common field to individual placodes. *Dev. Biol.* **276**, 1-15.
Sutherland, D., Samakovlis, C. and Krasnow, M. A. (1996). branchless encodes a Drosophila FGF homolog that controls tracheal cell migration and the pattern of branching. *Cell* **87**, 1091-1101.
Tomarev, S. I., Zinovieva, R. D., Chang, B. and Hawes, N. L. (1998). Characterization of the mouse Prox1 gene. *Biochem. Biophys. Res. Commun.* **248**, 684-689.
Tonou-Fujimori, N., Takahashi, M., Onodera, H., Kikuta, H., Koshida, S., Takeda, H. and Yamasu, K. (2002). Expression of the FGF receptor 2 gene (fgfr2) during embryogenesis in the zebrafish Danio rerio. *Gene Expr. Patterns* **2**, 183-188.
Torres, M., Gomez-Pardo, E. and Gruss, P. (1996). Pax2 contributes to inner ear patterning and optic nerve trajectory. *Development* **122**, 3381-3391.
Trokovic, N., Trokovic, R. and Partanen, J. (2005). Fibroblast growth factor signalling and regional specification of the pharyngeal ectoderm. *Int. J. Dev. Biol.* **49**, 797-805.
Westerfield, M. (2000). *The Zebrafish Book. A Guide for the Laboratory use of Zebrafish (Danio rerio).* Eugene: University of Oregon Press.
Wigle, J. T., Chowdhury, K., Gruss, P. and Oliver, G. (1999). Prox1 function is crucial for mouse lens-fibre elongation. *Nat. Genet.* **21**, 318-322.
Wright, T. J. and Mansour, S. L. (2003). Fgf3 and Fgf10 are required for mouse otic placode induction. *Development* **130**, 3379-3390.
Xu, P. X., Adams, J., Peters, H., Brown, M. C., Heaney, S. and Maas, R. (1999). Eya1-deficient mice lack ears and kidneys and show abnormal apoptosis of organ primordia. *Nat. Genet.* **23**, 113-117.
Xu, P. X., Zheng, W., Huang, L., Maire, P., Laclef, C. and Silvius, D. (2003). Six1 is required for the early organogenesis of mammalian kidney. *Development* **130**, 3085-3094.
Yang, X., Dormann, D., Munsterberg, A. E. and Weijer, C. J. (2002). Cell movement patterns during gastrulation in the chick are controlled by positive and negative chemotaxis mediated by FGF4 and FGF8. *Dev. Cell* **3**, 425-437.
Zhang, Y., Buchholz, F., Muyrers, J. P. and Stewart, A. F. (1998). A new logic for DNA engineering using recombination in Escherichia coli. *Nat. Genet.* **20**, 123-128.
Zheng, W., Huang, L., Wei, Z. B., Silvius, D., Tang, B. and Xu, P. X. (2003). The role of Six1 in mammalian auditory system development. *Development* **130**, 3989-4000.
Zou, D., Silvius, D., Fritzsch, B. and Xu, P. X. (2004). Eya1 and Six1 are essential for early steps of sensory neurogenesis in mammalian cranial placodes. *Development* **131**, 5561-5572.

Table S1. Downregulated genes

Gene name	Gene description	Chr. location			Fold changes
Tubule	Whole testis				
Ddx3y	DEAD (Asp-Glu-Ala-Asp) box polypeptide 3, Y-linked	Y	-157.6	-724.1	
Uty	ubiquitously transcribed tetratricopeptide repeat gene, Y chromosome	Y	-34.3	-4.0	
Eif2s3y	eukaryotic translation initiation factor 2, subunit 3, structural gene Y-linked	Y	-27.9	-97.0	
Jarid1d	jumonji, AT rich interactive domain 1D (Rbp2 like)	Y	-22.6	-5.3	
Nxf2	nuclear RNA export factor 2	X	-16.0	-12.1	
Tuba3	tubulin, alpha 3	6	-9.2	-19.7	
Dst	dystonin	1	-9.2	-4.3	
Clca1	chloride channel calcium activated 1	3	-7.5	-4.6	
Alcam	activated leukocyte cell adhesion molecule	16	-5.7	-2.1	
Apod	apolipoprotein D	16	-5.3	-2.8	
Kctd14	potassium channel tetramerisation domain containing 14	7	-5.3	-2.3	
Slc6a4	solute carrier family 6 (neurotransmitter transporter, serotonin), member 4	11	-5.3	-2.1	
1190002H23Rik	RIKEN cDNA 1190002H23 gene	14	-4.6	-4.0	
Jam2	junction adhesion molecule 2	16	-4.6	-2.6	
Scara5	scavenger receptor class A, member 5 (putative)	14	-4.6	-2.6	
Ube1y1	ubiquitin-activating enzyme E1, Chr Y 1	Y	-3.7	-7.0	
9630031F12Rik	RIKEN cDNA 9630031F12 gene	5	-3.5	-3.0	
Rab3b	RAB3B, member RAS oncogene family	4	-3.5	-2.1	
Nfkbiz	nuclear factor of kappa light polypeptide gene enhancer in B-cells inhibitor, zeta	16	-3.2	-2.5	
Plod2	procollagen lysine, 2-oxoglutarate 5-dioxygenase 2	9	-3.2	-2.1	
Morc1	microrchidia 1	16	-3.0	-7.0	
BC022960	cDNA sequence BC022960	X	-3.0	-3.0	
Trim7	tripartite motif protein 7	11	-3.0	-2.1	
Cxcr4	chemokine (C-X-C motif) receptor 4	1	-2.8	-2.8	
Dusp15	dual specificity phosphatase-like 15	2	-2.8	-2.0	
Apoa2	apolipoprotein A-II	1	-2.6	-4.6	
Id4	inhibitor of DNA binding 4	13	-2.6	-3.2	
Cd83	CD83 antigen	13	-2.6	-2.5	
Ehd1	EH-domain containing 1	19	-2.6	-2.3	
3230401M21Rik	RIKEN cDNA 3230401M21 gene	18	-2.5	-2.3	
MGI:1916782	homeobox only domain	5	-2.5	-2.1	
Bcl7c	B-cell CLL/lymphoma 7C	7	-2.5	-2.0	
Dtymk	deoxythymidylate kinase	1	-2.3	-2.8	
Cp	ceruloplasmin	3	-2.3	-2.5	
Foxq1	forkhead box Q1	13	-2.3	-2.1	
Tyro3	TYRO3 protein tyrosine kinase 3	2	-2.3	-2.0	
Hells	helicase, lymphoid specific	19	-2.1	-7.0	
Ris2	retroviral integration site 2	8	-2.1	-2.6	
Gadd45b	growth arrest and DNA-damage-inducible 45 beta	10	-2.1	-2.5	
Edn1	endothelin 1	13	-2.1	-2.3	
Stk4	serine/threonine kinase 4	2	-2.1	-2.3	
Galnt7	UDP-N-acetyl-alpha-D-galactosamine: polypeptide N-acetylgalactosaminyltransferase 7	7	8	-2.1 -2.0	
Rarres2	retinoic acid receptor responder (tazarotene induced) 2	6	-2.1	-2.0	
Zcchc3	zinc finger, CCHC domain containing 3	2	-2.0	-3.2	
Ctnnal1	catenin (cadherin associated protein), alpha-like 1	4	-2.0	-2.3	
Plagl1	pleiomorphic adenoma gene-like 1	10	-2.0	-2.3	
1300007B12Rik	RIKEN cDNA 1300007B12 gene	1	-2.0	-2.1	
4930588M11Rik	RIKEN cDNA 4930588M11 gene	3	-2.0	-2.1	

Table S2 Up-regulated genes

Gene name	Gene description	Chr. location	Fold changes	
			Tubule	Whole testis
Xist	inactive X specific transcripts	X	48.5	27.9
Klk16	kallikrein 16	7	24.3	7.5
Asb12	ankyrin repeat and SOCS box-containing protein 12	X	17.1	2.5
Sult1e1	sulfotransferase family 1E, member 1	5	14.9	7.0
Klk6	kallikrein 6	7	14.9	4.0
Col9a3	procollagen, type IX, alpha 3	2	13.0	4.6
Rhbg	Rhesus blood group-associated B glycoprotein	3	12.1	3.7
Klk27	kallikrein 27	7	9.8	4.9
Myh6	myosin, heavy polypeptide 6, cardiac muscle, alpha	14	9.8	3.0
D16Bwg1494e	DNA segment, Chr 16, Brigham & Women's Genetics 1494 expressed	16	9.2	4.0
FHOS2	formin-family protein FHOS2	18	9.2	3.2
Snrpn	small nuclear ribonucleoprotein N	7	9.2	2.8
Klk24	kallikrein 24	7	8.6	7.0
Cps1	carbamoyl-phosphate synthetase 1	1	8.0	8.6
Stom	stomatin	2	8.0	2.3
Klk22 /// Klk9	kallikrein 22 /// kallikrein 9	7	7.5	6.5
Svs5	seminal vesicle secretion 5	2	7.5	3.2
Htatip2	HIV-1 tat interactive protein 2, homolog (human)	7	7.5	2.3
Glb1	galactosidase, beta 1	9	7.0	2.5
Klk21	kallikrein 21	7	6.5	6.5
Thrsp	thyroid hormone responsive SPOT14 homolog (Rattus)	7	6.5	4.9
Abcb1a	ATP-binding cassette, sub-family B (MDR/TAP), member 1A	5	6.5	2.8
RIKEN cDNA 1100001H23	1100001H23Rik	6	6.5	6.5
Slc39a8	solute carrier family 39 (metal ion transporter), member 8	3	6.1	4.3
Akr1c12	aldo-keto reductase family 1, member C12	13	6.1	2.0
Spp1	secreted phosphoprotein 1	5	5.7	5.3
Gpx7	glutathione peroxidase 7	4	5.7	2.3
Anxa3	annexin A3	5	5.7	2.0
Asb9	ankyrin repeat and SOCS box-containing protein 9	---	5.3	2.5
Masp1	mannan-binding lectin serine peptidase 1	16	4.9	2.6
Klk1	kallikrein 1	7	4.6	5.7
A930025J12Rik	RIKEN cDNA A930025J12 gene	5	4.6	4.0
Hsd17b3	hydroxysteroid (17-beta) dehydrogenase 3	---	4.0	2.1
Ephx1	epoxide hydrolase 1, microsomal	1	3.7	2.3
Rcn1	reticulocalbin 1	2	3.7	2.1
LOC544986	similar to hypothetical protein LOC67055	14	3.5	3.2
Kit	kit oncogene	5	3.5	2.0
Vnn1	vanin 1	10	3.2	4.0
Mbp	myelin basic protein	18	3.2	2.8
Hsd3b1	hydroxysteroid dehydrogenase-1, delta<5>-3-beta	3	3.2	2.5
Akr1c13	aldo-keto reductase family 1, member C13	13	3.2	2.3
Itih2	inter-alpha trypsin inhibitor, heavy chain 2	2	3.2	2.3
Pcolce	procollagen C-endopeptidase enhancer protein	5	3.2	2.0
Rdh11	retinol dehydrogenase 11	12	3.0	3.7
Wnt5a	wingless-related MMTV integration site 5A	14	3.0	2.8
4933407N01Rik	RIKEN cDNA 4933407N01 gene	11	3.0	2.3
Plxnd1	Plexin D1 (Plxnd1), mRNA	6	3.0	2.3
Txk	TXK tyrosine kinase	5	3.0	2.3
Zfp185	zinc finger protein 185	X	3.0	2.0
Tnfrsf12a	tumor necrosis factor receptor superfamily, member 12a	17	2.8	2.8
Tcn2	transcobalamin 2	11	2.8	2.6
Plp1	proteolipid protein (myelin) 1	X	2.8	2.5
MGI:1889205	plasma glutamate carboxypeptidase	15	2.8	2.1
Cd36	CD36 antigen	5	2.8	2.0
Slc39a8	solute carrier family 39 (metal ion transporter), member 8	3	2.6	5.7
Synpo	synaptopodin	18	2.6	3.5
Bscl2	Bernardinelli-Seip congenital lipodystrophy 2 homolog (human)	19	2.6	3.0
Frzb	frizzled-related protein	2	2.6	2.5
Car4	carbonic anhydrase 4	11	2.6	2.1
Cyp2d22	cytochrome P450, family 2, subfamily d, polypeptide 22	---	2.6	2.1
Pcolce	procollagen C-endopeptidase enhancer protein	5	2.6	2.1
Txndc5	thioredoxin domain containing 5	13	2.6	2.1
2310016C16Rik	RIKEN cDNA 2310016C16 gene	13	2.6	2.0
Myadm	myeloid-associated differentiation marker	7	2.6	2.0
Pld3	phospholipase D family, member 3	7	2.6	2.0
Olig1	oligodendrocyte transcription factor 1	16	2.5	2.6
Hfe	hemochromatosis	13	2.5	2.5
Tceal3	transcription elongation factor A (SII)-like 3	X	2.5	2.5
4632428N05Rik	RIKEN cDNA 4632428N05 gene	10	2.5	2.3
Ctps2	cytidine 5′-triphosphate synthase 2	X	2.5	2.3
Trp53inp1	transformation related protein 53 inducible nuclear protein 1	4	2.5	2.3
Sesn3	sestrin 3	9	2.5	2.1
Ndrg4	N-myc downstream regulated gene 4	8	2.5	2.0
septin 6	37504	X	2.5	2.5
Dnaja4	DnaJ (Hsp40) homolog, subfamily A, member 4	9	2.3	4.0
Slc25a29	solute carrier family 25, member 29	12	2.3	2.8
Bbox1	butyrobetaine (gamma), 2-oxoglutarate dioxygenase 1	2	2.1	5.3
Atp6v0e2	ATPase, H+ transporting, lysosomal, V0 subunit E isoform 2	6	2.1	2.3
Dspg3	dermatan sulphate proteoglycan 3	10	2.1	2.3
Mdfic	MyoD family inhibitor domain containing	6	2.1	2.0
9530028C05	hypothetical protein 9530028C05	6	2.0	5.3
A130022J15Rik	RIKEN cDNA A130022J15 gene	6	2.0	2.8
Acacb	acetyl-Coenzyme A carboxylase beta	5	2.0	2.8
Dap	death-associated protein	15	2.0	2.8
Utx	ubiquitously transcribed tetratricopeptide repeat gene, X chromosome	X	2.0	2.8
Vcam1	vascular cell adhesion molecule 1	3	2.0	2.8
Gpx3	glutathione peroxidase 3	11	2.0	2.6
Sc5d	sterol-C5-desaturase homolog	9	2.0	2.5
Tmem71	ransmembrane protein 71	15	2.0	2.5
Fkbp9	FK506 binding protein 9	6	2.0	2.1
Acsl6	acyl-CoA synthetase long-chain family member 6	11	2.0	2.0
Actn3	actinin alpha 3	19	2.0	2.0
Lmo2	LIM domain only 2	2	2.0	2.0